THE PENNSYLVANIA STATE UNIVERSITY
SCHREYER HONORS COLLEGE

DEPARTMENT OF BIOCHEMISTRY AND MOLECULAR BIOLOGY

How Does NfuA Regenerate a [4Fe-4S] Cluster in Lipoyl Synthase?

JAY PENDYALA
SPRING 2021

A thesis
submitted in partial fulfillment
of the requirements
for a baccalaureate degree in Biochemistry and Molecular Biology
with honors in Biochemistry and Molecular Biology

Reviewed and approved* by the following:

Amie K. Boal
Associate Professor of Chemistry
Associate Professor of Biochemistry and Molecular Biology
Thesis Supervisor

Joseph C. Reese
Associate Department Head for Research and Faculty Development
Professor of Biochemistry and Molecular Biology
Honors Adviser

* Electronic approvals are on file.

ABSTRACT

Lipoyl synthase (LipA) sacrifices its auxiliary 4Fe-4S cluster to insert two sulfur atoms at carbons C6 and C8 of an octanoyl peptide substrate. This step completes the biosynthesis of lipoic acid, an essential enzyme cofactor for aerobic metabolism. In principle, the sacrificial nature of LipA's mechanism limits its ability to perform multiple turnovers. However, another iron sulfur carrier protein, NfuA, reassembles LipA's auxiliary cluster to enable multi-turnover activity in *Escherichia coli* (*Ec*). Moreover, the N-terminal domain of *Ec* NfuA has been shown to be essential for tight interaction with *E. coli* LipA, thereby facilitating multiple turnovers. NfuA's conserved C-terminal Fe-S cluster binding motif, CXXC, facilitates the regeneration of the auxiliary Fe-S cluster in LipA. In the human NfuA homolog, NFU1, a glycine to cysteine mutation, G208C, near the CXXC motif is lethal. This mutation impairs lipoic acid synthase (LAS) and the activity of the pyruvate dehydrogenase complex (PDHC). Here, we seek to understand the mechanism of NfuA-mediated cluster transfer via characterization of a thermophilic homolog from *Thermosynechococcus elongatus* (*Te*). Unlike *Ec* NfuA (21 kDa), *Te* NfuA (12 kDa) doesn't carry an A-type N-terminal domain. To study the LipA-NfuA interaction via activity and binding assay, we used four *T. elongatus* proteins including LipA wild-type (wt), NfuA wt, a fusion of *Ec* NfuA N-term/ *Te* NfuA, and *Te* NfuA G55C. We also propose Mössbauer spectroscopy and crystallography studies of *Te* NfuA to address a long-standing gap in knowledge about this important iron-sulfur cofactor chaperone. Achieving these objectives will be useful to studying the properties of clinically relevant variants.

TABLE OF CONTENTS

LIST OF FIGURES

LIST OF TABLES

ACKNOWLEDGEMENTS

I would like to thank the Penn State Schreyer Honors College and the Biochemistry and Molecular Biology department for providing the resources and opportunities to challenge myself and grow as an undergraduate scholar. I would like to thank the Erickson Discovery Grant Program, Eberly's Undergraduate Research Support, and Student Engagement Network for their generous financial support of my research. I am thankful to Dr. Scott Showalter whose honors chemistry course and my first introduction to laboratory research taught me incredible lessons about myself and how I wanted to learn. I am grateful for my honors advisor, Dr. Joseph Reese, who is always accessible and welcoming to provide valuable academic advise. Although I wasn't formally a member in his lab, my project is an extension of the highly impactful research done by Dr. Squire Booker and Dr. Erin McCarthy. Dr. Booker was especially helpful in improving my presenting skills during the Beckman Scholars application. Finally, I come to the members of the Boal Group. I am indebted to José del Río-Pantoja for introducing me to the lab and my fellow undergraduate and graduate students for creating a positive environment and making the bench an enjoyable place to work and communicate. I can't express enough appreciation for Dr. Amie Boal and Vivian Robert Jeyachandran, who in my eyes are the best scientists and role models. Dr. Boal your integrity, wisdom, and kind-hearted nature are truly inspiring qualities. Emulating your prose has single-handedly, taken my academic writing to the next level and your communication skills are forever invaluable. Vivian your intelligence, patience, and perseverance are unparalleled. You always consider my ideas and questions, no matter how incorrect or juvenile they may seem at times. You helped me rationalize challenging concepts and data which ultimately improved my critical thinking and experimental skills. I am proud to have been mentored by Dr. Boal and Vivian. Finally, I thank all my friends and family for their continued support. You are all my greatest asset.

Chapter 1: Introduction

1.1 Lipoyl Synthase Structure and Function

Significance of Lipoic Acid (LA)

Aberrations in the biosynthesis of LA can yield a plethora of harmful health outcomes such as mitochondrial diseases, prompting the holistic review of the key factors in such pathways.[29,31] LA is a virtually ubiquitous sulfur-containing enzyme cofactor among organisms capable of undergoing aerobic metabolism. Two pathways exist for the cofactor's biosynthesis: a salvage pathway and a *de novo* biosynthetic route. Many organisms, ranging from simple bacteria [*Escherichia coli (E. coli)*] to higher eukaryotes [*Homo sapiens (H. sapiens)*], possess both pathways.[21] In the two-step salvage pathway, scavenged free lipoic acid is then activated via adenylation to generate lipoyl-AMP and inorganic pyrophosphate. The lipoyl group is transferred to a lipoyl carrier protein (LCP) with the release of AMP (Figure 1). In *E. coli* (*Ec*) and many other bacteria, both reactions are carried out by one polypeptide, lipoate protein ligase A (LplA).[27] In mammals and some prokaryotes, these functions are split between a lipoate-activating enzyme and a lipoyl transferase. The *de novo* pathway involves a two-step process that branches from the type II fatty acid biosynthetic pathway. The first step, catalyzed by octanoyl transferase (LipB), is the transfer of an *n*-octanoyl chain from octanoyl-acyl carrier protein (ACP) to an LCP.[14, 39] The second enzyme, LipA, catalyzes the stepwise insertion of sulfur at C6 and C8 of the octanoyl chain, yielding the final cofactor (Figure 1). The LA created from these pathways has antioxidant properties and is a key regulator of cell signaling pathways (i.e., regulation of the transcription factor NF-κB).[31] Given its essentiality, LA is a prominent target in the treatment of disorders induced by oxidative stress such as diabetic neuropathy, multiple sclerosis, and Alzheimer's disease.

The LA salvage pathway is notably absent in *Mycobacterium tuberculosis* (*M. tuberculosis*), the bacterium that causes tuberculosis. This feature of *M. tuberculosis (Mt)* motivates detailed study of the de novo pathway because the enzymes involved could be exploited as drug targets, given that this pathway is the sole source of the essential LA cofactor. Genomic

analysis reveals that LA is attached to three distinct *Mt* metabolic protein complexes: the H protein (GcvH) of the glycine cleavage system, and the E2 subunits of the α-ketoglutarate (KDH) and pyruvate dehydrogenase (PDH) complexes.[16,26] The H-protein catalyzes the reductive amination of glyoxylate to glycine, a constituent of the peptidoglycan layer in the bacterial cell wall. The lipoyl groups of KDH and PDH act as a 14 Å appendage to catalyze oxidative decarboxylation of their respective substrates.[16] These reactions produce NADH, the initial electron source to generate ATP through the electron transport chain. Thus, genes involved in LA *de novo* biosynthesis are vital for *Mt's* survival in the early stages an infection that according to the World Health Organization has affected one-third of the world's population. Consequently, their protein products may serve as efficacious drug targets against extensively drug-resistant strains of *Mt*. One such target is the LipA enzyme as it is the source of the sulfurs which provide the oxidative features of the metabolic multi-enzymes. Hence, an appropriate understanding of LipA's structure and function is imperative in the development of antituberculosis drugs. Specific questions to answer would be the mechanism of sulfur insertion into LA, how the sulfur source in LipA is recycled to promote LipA activity, and the effect that mutations in lipoic biosynthesis have on LipA activity.

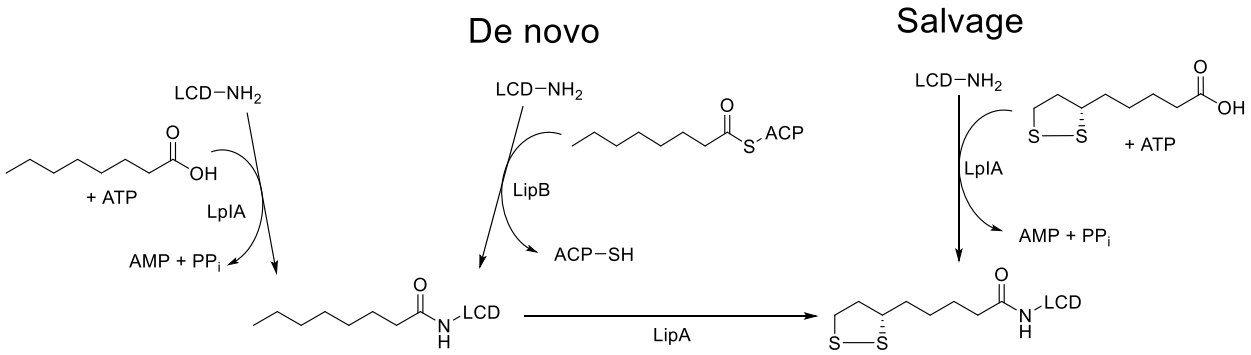

Figure 1. De novo and salvage pathways of lipoic acid biosynthesis.

Background

LipA is a radical SAM (RS) enzyme.[3] RS enzymes constitute a superfamily of structurally and mechanistically related metalloproteins that use SAM to initiate a multitude of radical-dependent transformations. All characterized RS enzymes (ie. LipA, BioB, and MiaB) that catalyze sulfur insertion have at least two iron-sulfur (Fe-S clusters).[3, 10] A significant body of evidence indicates that the one of these clusters are degraded during catalysis to supply the attached sulfur atoms. In the absence of other components to reconstitute the cluster, this strategy limits

these proteins to catalyzing only a single turnover. Given the therapeutic value of LipA mediated LA biosynthesis, we aim to build on current knowledge to characterize LipA's multi-turnover activity. Here, we review previous studies of LipA structure and function in which spectroscopic, biochemical, and structural experiments were used to characterize LipA's generation of LA. These prior projects employed the bacterial *Ec*, *Mt*, and *Thermosynechococcus. elongatus* (*T. elongatus*) LipA systems.

Determining the source of the sulfur atoms in LA biosynthesis

Ultraviolet-visible (UV-VIS) and Mössbauer spectroscopy reveal two distinct $[4Fe\text{-}4S]^{2+}$ clusters per *Ec* LipA polypeptide.[6] UV-Vis spectroscopy uses UV-vis electromagnetic radiation (800-200 nm wavelengths) to excite electrons from the ground state to the first singlet excited state of the compound to quantitively determine different analytes, such as transition metal ions and biological macromolecules.[1] The UV-Vis spectrum of the as-isolated (AI) and reconstituted *Ec* LipA wild-type (wt) enzymes show the expected 415-400 nm shoulder of a 4Fe-4S cluster containing protein (Figure 2a). Mössbauer spectroscopy employs gamma (γ) radiation and a detector the measure the intensity of the beam transmitted through the sample. The atoms in the source emitting the γ rays must be the same isotope as the atoms in the sample absorbing them allows the nuclear transition energies of the source and sample to be equal. However, if the sample isotope is in a different chemical environment, the nuclear levels shift on a scale of micro-electronvolts (mEv).[12, 32] To bring the two nuclei back into resonance it is necessary to change the energy of the γ ray as the source is accelerated through a range of velocities. The resulting spectra plots γ ray intensity as a function of the source velocity. At velocities corresponding to the resonant energy levels of the sample, a fraction of the gamma rays is absorbed, resulting in a drop in the measured intensity and a corresponding peak in the spectrum. The number, positions, and intensities of the peaks provides information regarding the oxidation states, spins (correlated to bond length), and ligand information of the sample isotope. This technique requires use of ^{57}Fe labeling for analysis of Fe/S cofactors. It has been reported that the AI wt LipA enzyme contained 6.9 ± 0.5 irons and 6.4 ± 0.9 sulfides per polypeptide. Mössbauer spectroscopy of the ^{57}Fe and sodium sulfide reconstituted wt enzyme contained 9.2 ± 0.4 irons and 8.8 ± 0.1 sulfides corresponding to two $[4Fe\text{-}4S]^{2+}$ clusters per polypeptide, with the remainder of the iron occurring as adventitiously bound species (Figure 2B).[6] One cluster is ligated by the cysteine amino acids in

the CX_3CX_2C motif that is common to all radical SAM enzymes, while the other is ligated by the cysteine amino acids residing in a CX_4CX_5C motif, which is conserved only in lipoyl synthases.[6] The C68A-C73A-C79A triple variant, expressed and isolated under identical conditions, contained 3.0 ± 0.1 irons and 3.6 ± 0.4 sulfides per polypeptide, while the C94A-C98A-C101A triple variant contained 4.2 ± 0.1 irons and 4.7 ± 0.8 sulfides per polypeptide. Mössbauer spectroscopy of the as-isolated wild-type protein and the two triple variants indicates that greater than 90% of all associated iron is found in the two $[4Fe\text{-}4S]^{2+}$ clusters.[6]

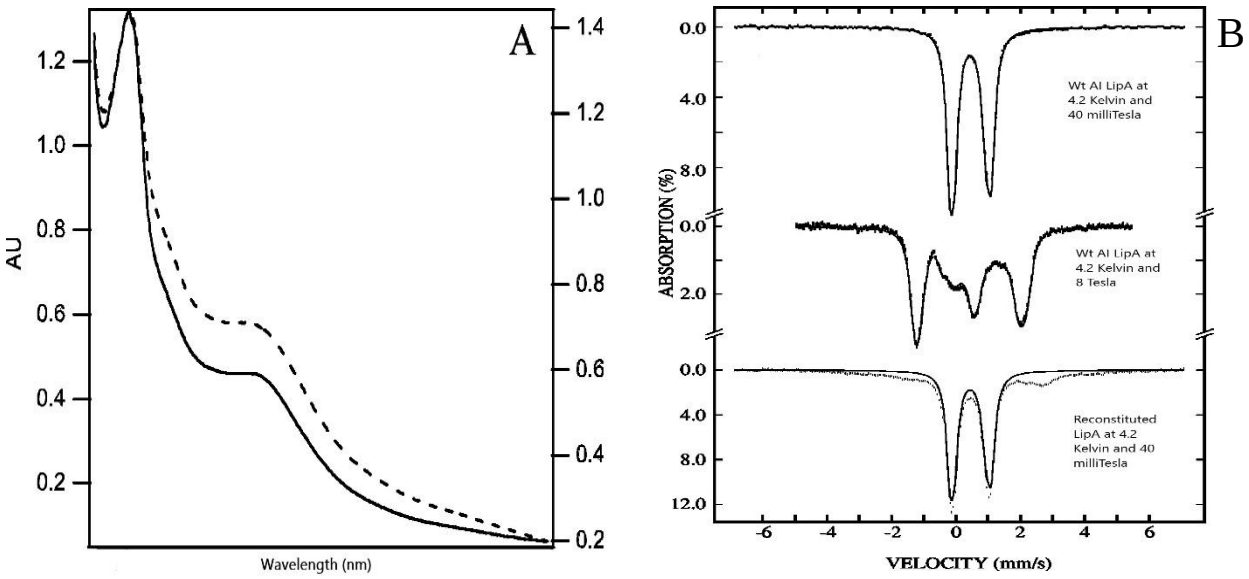

Figure 2. A) UV-visible spectra of Wt LipA; B) Mössbauer spectra of Wt AI LipA recorded at 4.2 K in an externally applied field 40 mT (top panel), 8 T (middle panel) reconstituted Wt LipA at 4.2 K and 40 mT.[6]

LA's sulfurs are derived from Ec LipA

Once it was established that each LipA harbors two $[4Fe\text{-}4S]^{2+}$ clusters, researchers used ^{34}S labelling to determine if the dithiolation originates from sulfide ions associated with the iron-sulfur clusters in LipA.[8] To answer this question, *Ec* LipA was grown in minimal medium with $Na_2{}^{34}S$ as the only sulfur source for comparison to samples grown in solely in natural Na_2S. Enzymatic turnover experiments were performed in the absence of extraneous sources of sulfur and equimolar concentrations of ^{34}S- and ^{32}S-labelled *Ec* LipA. Liquid chromatography coupled to mass spectrometry (LC-MS) indicate similar relative intensities of lipoyl cofactor containing either two atoms of ^{32}S or of ^{34}S, which is consistent with the notion that both sulfurs originate from the same polypeptide without release of monothiolated intermediates.[8] If alternative

mechanisms were in play, the isolated lipoyl cofactor should contain a 1:2:1 ratio of ^{32}S-^{32}S, ^{32}S-^{34}S, and ^{34}S-^{34}S, respectively. This finding provides the basis to structurally characterize LipA's mechanism.[8]

As a metalloenzyme, one of LipA's Fe-S clusters provides an electron to cleave SAM into L-methionine and a 5'-deoxyadenosyl radical (5′-dA•).[5] In previous studies, activity assays using 100 μM deuterium labelled [octanoyl-d_{15}]H protein (OHP) substrate, 50 μM *Ec* LipA, and 700 μM SAM showed that the 5′-dA• acts directly on the octanoyl substrate to abstract the deuterium and produce a [lipoyl]H protein (LHP). This finding aligns with the predetermined model that removal of hydrogen atoms from carbons 6 (C6) and 8 (C8) of the octanoyl chains is a prerequisite for sulfur insertion. Subsequent studies, in which only C8 is specifically labeled with deuterium in significant suppression of lipoyl product formation and that sulfur insertion at C6 always precedes insertion at C8, even with an unlabeled substrate. Moreover, an unlabeled reaction screening for the formation of 5'-dA and LHP suggested that 2 equivalents of SAM are cleaved to produce 1 equivalent of LHP (Table 1, Figure 3).[7] The amplitudes of each plot reveal the maximum amount 5′- dA formed was 50.5 μM which corresponds to 1.01 equiv with respect to 50 μM LipA, and 18.4 μM LHP, which corresponds to 0.378 equiv. The product concentrations of 5'-dA to LHP range from 2.38 at early time points to 2.71 at later time points. These ratios can be rationalized by a mechanism in which 2 equivalents of both SAM and LipA are required to synthesize LHP from OHP if a given fraction of 5′-dA results from nonproductive cleavage of SAM.[7]

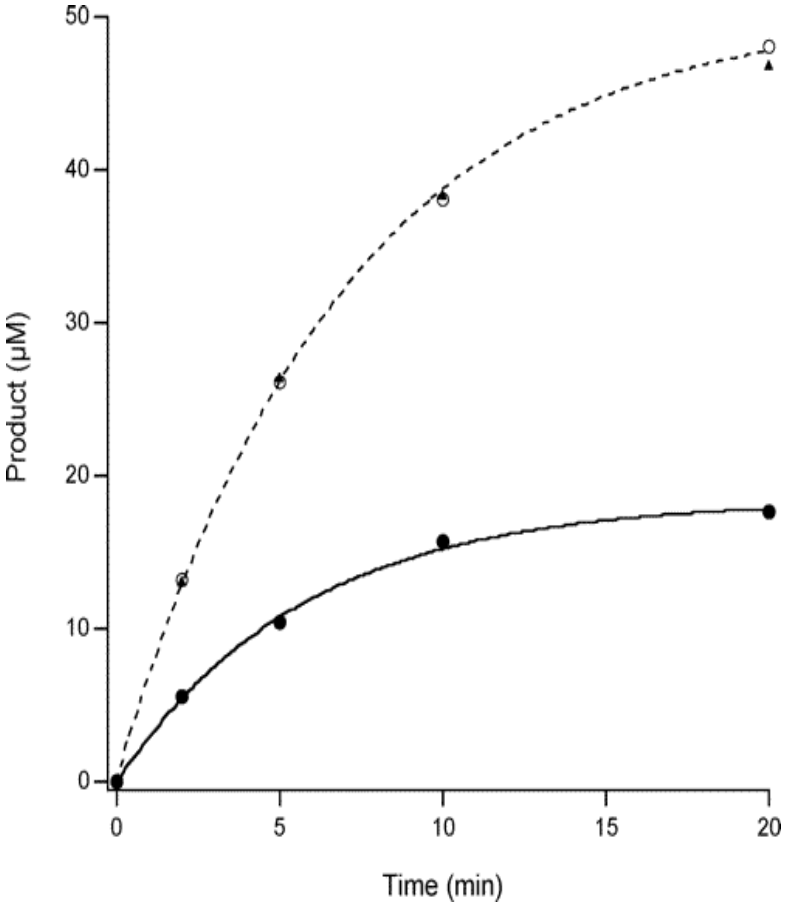

Table 1. Time-Dependent Formation of 5′-dA and LHP				
Time (min)	5′-dA (μM) (observed)	5′-dA (μM) (computed)	LHP (μM)	5′-dA/LHP
0	0	0	0	N/A
2	13.2	13.1	5.54	2.38
5	26.1	26.4	10.4	2.51
10	38.0	38.4	15.7	2.42
2-	48.0	46.8	17.7	2.71

Figure 3. Stoichiometry ratios of 5'-dA to LHP support the model in which 2 equivalents of AdoMet and *Ec* LipA are required to synthesize LHP from OHP.[7] Time-dependent formation of lipoyl product (solid line) and 5'-dA (dashed line).

LipA uses radical chemistry for sulfur insertion

The intramolecular reductive cleavage of SAM and the subsequent abstraction of the substrate's C6 hydrogen yields a radical intermediate.[17, 18] Incorporating deuterium at C8 of a target (N6-octanoyl)-lysyl residue in a synthetic tripeptide substrate significantly impeded formation of the lipoyl group and chemically supported an intermediate in which sulfur insertion at C6 precedes insertion at C8.[17] Given the slow rate of insertion of the second sulfur atom, use of only 1 equivalent of SAM with respect to enzyme concentration in a reaction with excess peptide substrate should result in the formation of an intermediate that cannot proceed to product. Mössbauer characterization of the trapped intermediate shows formation of a species with spectroscopic properties similar to those of other well-studied $[3Fe{-}4S]^0$ clusters.[32] The proposed structure of the intermediate (Figure 4) offers insight into how LipA's catalytic mechanism

proceeds. In the first half-reaction, SAM bound to the $[4Fe{-}4S]^{2+}$ cluster ligated by the CX_3CX_2C motif, noted as the radical SAM (RS) cluster, is reductively cleaved to a 5′-dA•, which is used to abstract an H• from C6 of the octanoyl chain. The resulting carbon radical attacks an activated form of the sulfide of the [4Fe−4S] cluster ligated by the CX_4CX_5C termed as the auxiliary cluster.[9, 11] In the second half-reaction, another equivalent of 5′- dA• is similarly generated, but it abstracts an H• from C8 of the octanoyl chain. The carbon radical at C8 attacks a second form of activated sulfide, presumably from the same auxiliary cluster. [9,11] Upon addition of two protons, the lipoyl cofactor is formed in its two-electron reduced state. This mechanism is consistent with the finding that the protein itself is the source of the inserted sulfur atoms and that both sulfurs derive from the same polypeptide.[11]

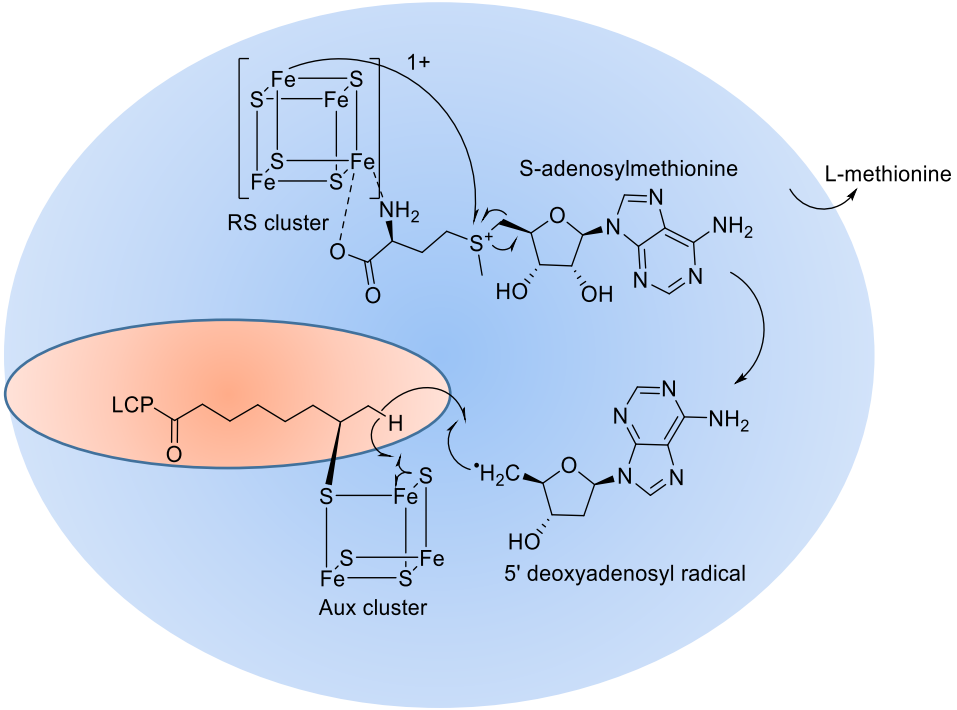

Figure 4. Proposed structure of LipA monothiolated intermediate.

Crystallographic experiments support the proposed LipA mechanism

Until recently, the aforementioned mechanism was only validated via spectroscopic and biochemical experiments. Crystallographic snapshots of *Mt* LipA's resting and intermediate states provided additional support for the proposed reaction pathway.[25] Figure 5a shows the substrate-free *Mt* LipA x-ray structure, in which the auxiliary cluster is sandwiched between N and C terminal domains of the polypeptide.[25] Three irons of the cuboidal cluster are coordinated by the

three cysteines (C) in the N-terminal CX_4CX_5C and the fourth iron attached to the C-terminal domain by serine 292 (S292) in a conserved RSSY motif.[25] Arginine 290 in this motif, although not bound to iron, blocks access to the auxiliary cluster. A six-stranded partial TIM barrel fold, common to most radical SAM enzymes, binds the RS cluster by the CX_3CX_2C motif and is responsible for radical generation. The two clusters are separated by a 15 Å. The octanollysine peptide substrate is primarily anchored to the N- terminal domain by hydrogen bonding to insert itself into cavity between the two 4Fe-4S clusters.[25] In the intermediate structure, the S292 ligand no longer binds the 4th Fe, which is presumably lost as Fe^{2+}. The N-terminal extension and auxiliary cluster move closer to the barrel to decrease the distance between the clusters to 11.8 Å.[25] With the substrate bound, R290 hydrogen bonds to the carbonyl of the peptide to expose the auxiliary cluster active site. The peptide is positioned for the reaction through additional hydrogen binding between the peptide's acyl amide, alanine 58's backbone amine, and glycine 58's carbonyl oxygen. In this structure, the L-methionine, 5′-dA• and substrate are situated ideally for the reaction at C6 to occur. The second thiolation at C8 requires another reductive SAM cleavage to generate the C8 radical. With the loss of the first Fe^{2+}, the formation of a 3Fe-4S cross-linked intermediate species allows the C8 radical to access the closest remaining sulfur atoms. Figure 6 summarizes the overall mechanism.

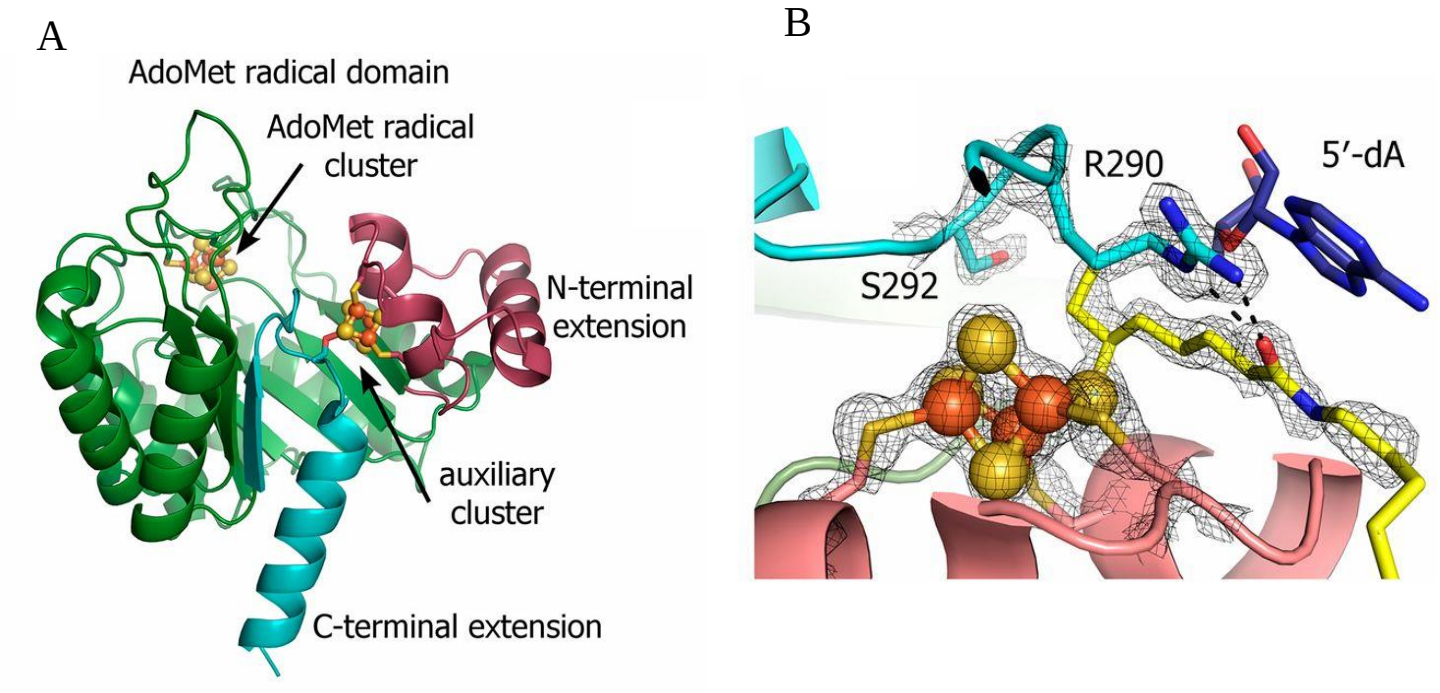

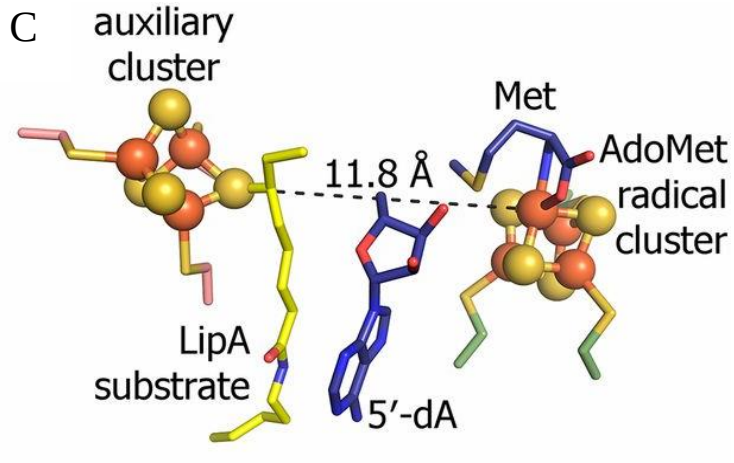

Figure 5. A) (top left) Substrate free *Mt* LipA in ribbon representation with the $(\beta/\alpha)_6$ AdoMet radical domain (green), N-terminal extension (red), and C-terminal extension (blue). **B)** (top right) The auxiliary cluster of *Mt* LipA with octanoyl-H peptide substrate (yellow), 5'-dA and methionine (blue). Simulated annealing omit density ($2F_o-F_c$) is contoured at 2.0σ in black mesh. **C)** (bottom left) Intermediate bound *Mt* LipA. The R290 residue is displaced allowing access to the auxiliary cluster.[25]

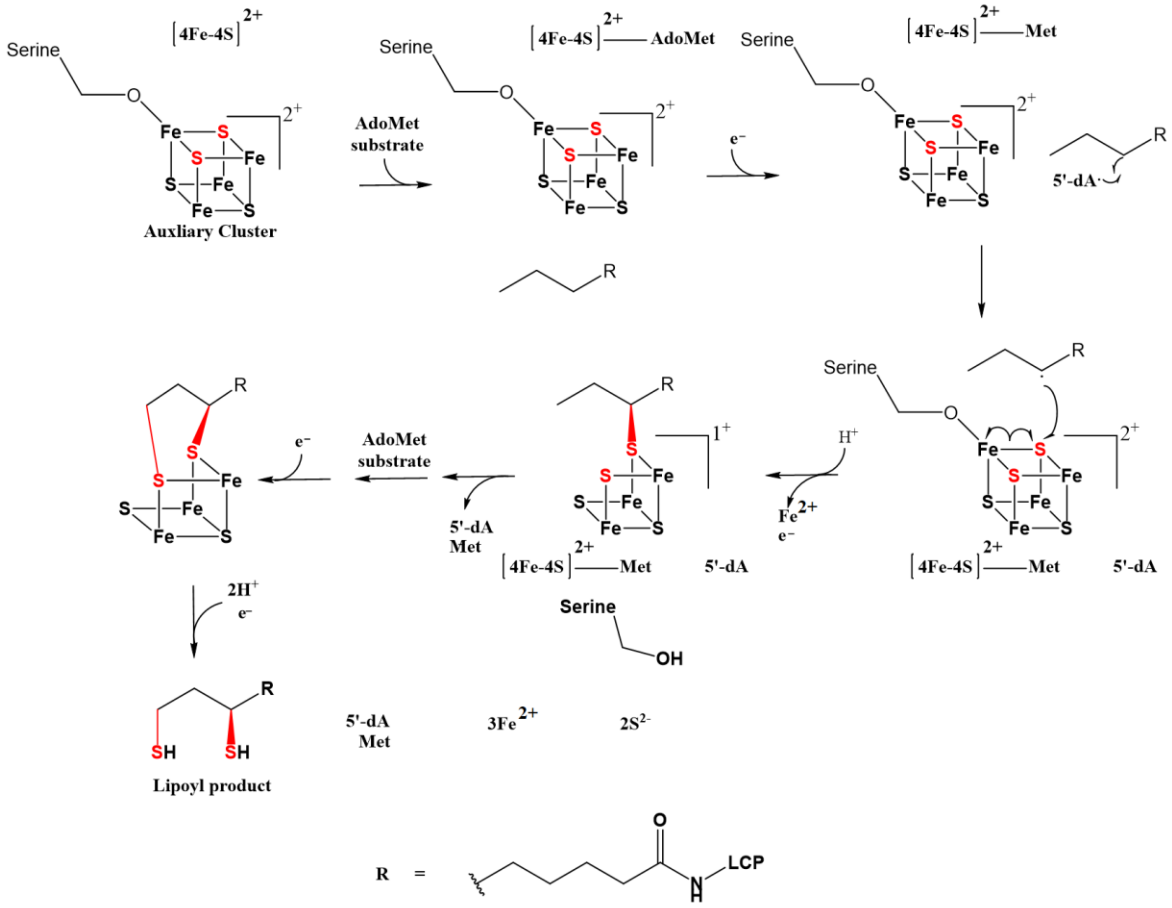

Figure 6. Mechanistic model LipA directed sulfur insertion in C6 and C8 of octanollysine peptide substrate.

This model of LipA catalysis shows that upon one complete turnover of C6 and C8 thiolation, four Fe^{2+} and two S^{2-} ions of the auxiliary cluster are released. Cannibalizing the auxiliary cluster renders LipA inactive, prompting the need to explore how the extra ions are handled and how the inactive form of LipA could be reactivated.[25] Possible explanations include the repair or replacement of the cluster - or simply accepting the system as single turnover with uncontrolled release of the free ferrous and sulfide ions. The last option could lead to inefficiency as well as iron and sulfide toxicity. It is thus unlikely. Alternatively, the regeneration of the auxiliary cluster by could be accomplished by the cellular iron sulfur cluster assembly machinery. The roles of proteins linked to this process in LipA catalysis were explored next.

1.2 NfuA reforms LipA's auxiliary cluster

Significance of NFU1

A missense mutation in exon 7 (c.622G>T) of the gene encoding human NfuA homolog, *NFU1*, was identified in ten individuals with pulmonary hypertension and neurological regression.[29] Unfortunately, these patients started exhibiting symptoms such as metabolic acidosis with variable acidemia and hyperglycemia and did not survive beyond 15 months.[16] Multi-sequence alignment of the conserved part of NFU1 protein shows that the missense mutation causes of a replacement of conserved glycine at 208 to cysteine. G208 is 2 residues upstream of the conserved Fe-S cluster binding CXXC motif.[29] The biochemical phenotype of the mutated individuals was consistent with aberrations in LA dependent pathways. Immunostaining with a lipoic acid specific antibody showed a 60% decrease in the E2 subunit of PDH due to defective lipoylation of octanoic acid substrate by LipA. These observations are consistent with an impairment of lipoic acid biosynthesis in *NFU1* mutated individuals.[29] Given that NFU1 functions as a vital maturation factor for a subset of mitochondrial Fe-S proteins, it was proposed that NFU1 might facilitate reassembly of the auxiliary cluster in LipA.

Size exclusion chromatography (SEC) analysis of NfuA suggests that one 4Fe-4S cluster bridges two monomers to create an active homodimer of NfuA.[22] To assess the stoichiometry of LA production when NfuA is included in the LipA reaction, activity assays were performed using 100 μM ^{34}S-labeled *Ec* NfuA, 20 mM *Ec* LipA (^{32}S), 600 mM peptide substrate analog, 0.5 mM SAH nucleosidase, 2 mM dithionite (DTT), and 1 mM SAM. More than 50% of lipoyl product contained two ^{32}S atoms which suggests that the remaining two sulfides of the auxiliary cluster

were used in a second turnover.[22] Formation of lipoyl product containing two ^{34}S atoms was detected after some lag. This observation suggests that NfuA's 4Fe-4S cluster was used to reconstitute LipA's auxiliary cluster.[22] When the reaction was replicated using excess ^{34}S-labeled *Ec* NfuA (400 mM), 1.5 equivalents of the ^{32}S-labeled lipoyl product was observed followed by production of multiple equivalents of the ^{34}S-labeled lipoyl product.[22] In another experiment, the addition of 5 mM citrate, a natural chelator of free iron, had no effect on NfuA's ability to enhance LipA turnover. These results indicate that NfuA directly reconstitutes LipA's auxiliary cluster.[22]

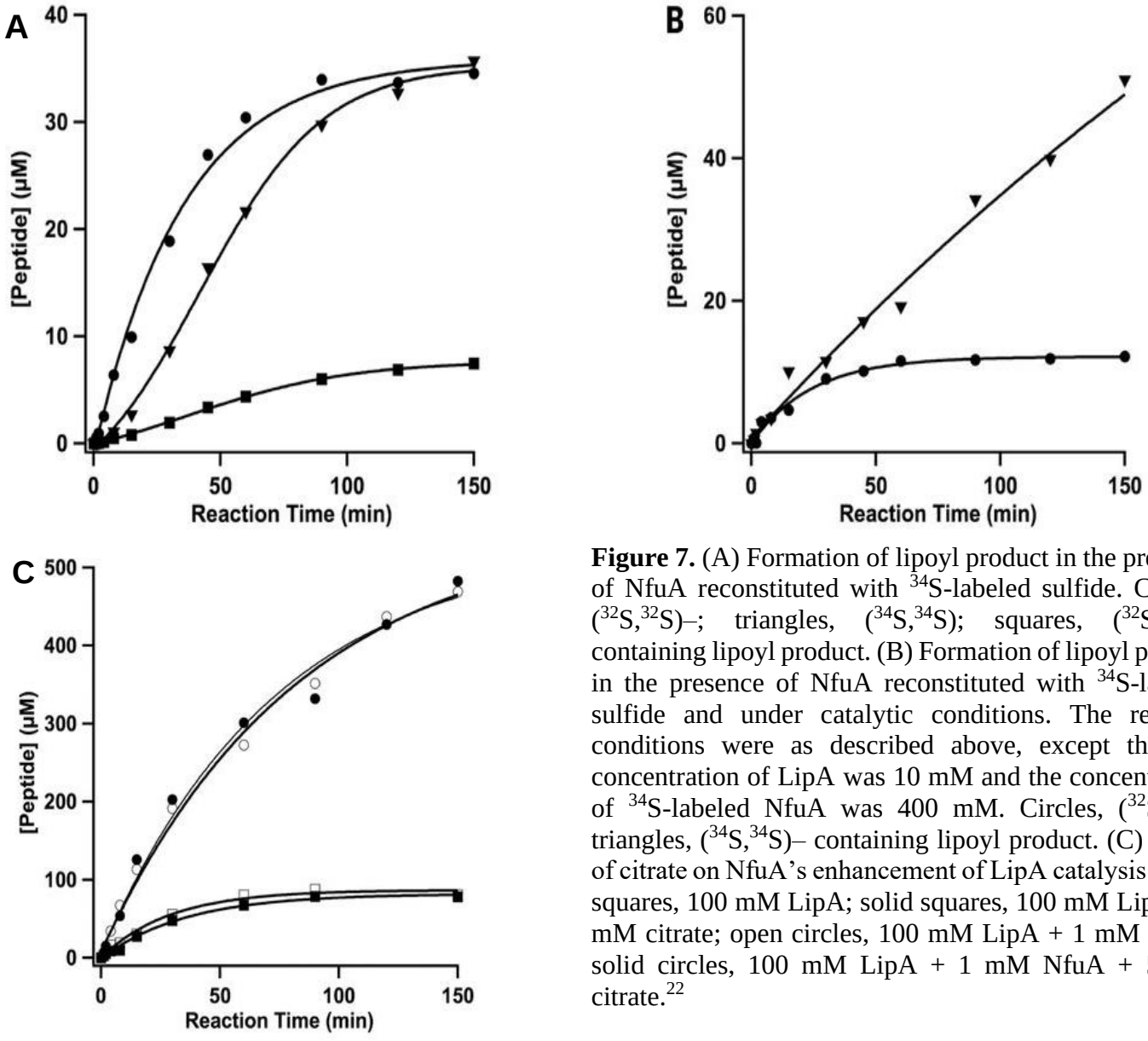

Figure 7. (A) Formation of lipoyl product in the presence of NfuA reconstituted with ^{34}S-labeled sulfide. Circles, (^{32}S,^{32}S)–; triangles, (^{34}S,^{34}S); squares, (^{32}S,^{34}S)– containing lipoyl product. (B) Formation of lipoyl product in the presence of NfuA reconstituted with ^{34}S-labeled sulfide and under catalytic conditions. The reaction conditions were as described above, except that the concentration of LipA was 10 mM and the concentration of ^{34}S-labeled NfuA was 400 mM. Circles, (^{32}S,^{32}S); triangles, (^{34}S,^{34}S)– containing lipoyl product. (C) Effect of citrate on NfuA's enhancement of LipA catalysis. Open squares, 100 mM LipA; solid squares, 100 mM LipA + 5 mM citrate; open circles, 100 mM LipA + 1 mM NfuA; solid circles, 100 mM LipA + 1 mM NfuA + 5 mM citrate.[22]

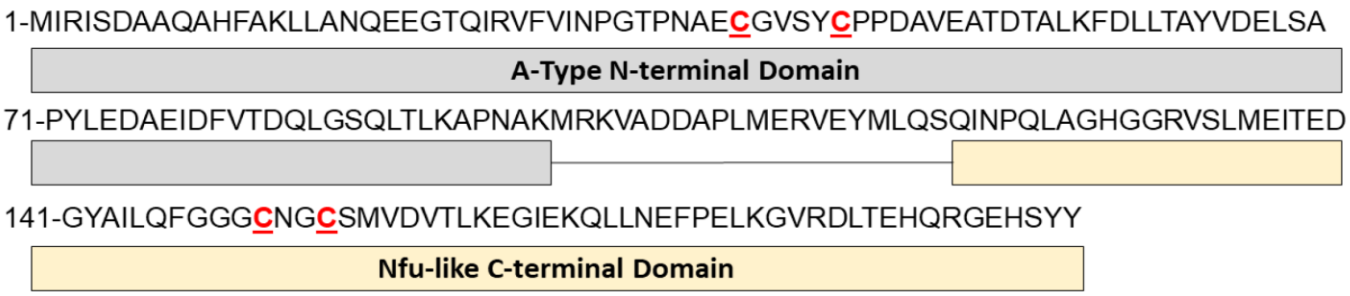

Figure 8. *E. coli* NfuA monomer sequence and domain structure.

The exact molecular mechanism of the NfuA-mediated cluster regeneration remains elusive however. Sequence comparisons show that *Ec* NfuA is composed of two distinct domains: a "degenerate" A-type N-terminal domain and an Nfu-like C-terminal domain. Both domains play a role in NfuA's function.[23] Site-direct mutagenesis and kinetic assays revealed that four cysteines, two in the N-terminal domain (C39 and C44) and two in the C-terminal domain (C149 and C152 of the CXXC motif) could coordinate the cluster transfer (Figure 8). While UV-vis absorption analysis of *Ec* NfuA's N-terminal domain alone showed no sign of Fe-S cluster interaction, mutating either C39 or C44 to an alanine (A) on the N-terminal domain resulted in reduced NfuA functionality. In fact, LA production was greatest when *Ec* LipA was combined with full-length wt *Ec* NfuA and lowest when *Ec* LipA was supplemented with just the *Ec* NfuA N-terminal domain. Experiments with two additional bacterial systems provide further support for the importance of NfuA's N-terminal domain.[23] With an 89% amino acid sequence similarity, *Mt* NfuA shares similar domain structure with *Ec* NfuA. As expected, *Ec* LipA has identical peptide production when coupled with *Mt* NfuA. *Staphylococcus aureus* (*S. aureus*) NfuA is homologous to *Ec* NfuA's C-terminal domain and when genetically fused with the *Ec* NfuA N-terminal domain, the fusion protein exhibited greater peptide production relative to wt *S. aureus* NfuA.[23] Expanding on this work, we sought to further characterize NfuA, its cofactors interaction with LipA, and the properties of clinically relevant NfuA variants.

1.3 Exploratory Questions Addressed in this Thesis

Given that robust multi-turnover activity has only been observed in the *Ec* LipA-NfuA system, we hope to identify other homologs that exhibit similar activity. Similarly, it was

established that some NfuA proteins lack an N-terminal domain. We want to understand whether these NfuAs are functional as LipA [4Fe-4S] cluster donors. One system that suits the aforementioned objectives is the LipA-NfuA system from a thermophilic cyanobacterium, *T. elongatus* (*Te*). *Te* NfuA lacks the N-terminal domain of NfuA (Figure 10). Presently, neither NfuA nor its interaction with LipA has been structurally characterized. Thermophilic proteins crystallize more easily and are more well-behaved. In fact, the *Te* LipA (PDB accession code 4U0P) crystal structure has been successfully solved already by another research group (Figure 9),[13] but its activity and interaction with NfuA are unknown. We will also evaluate the crystallization propensity of *Te* NfuA, both alone and in complex with LipA. Finally, we will examine the effects of a G→C substitution upstream of the C-terminal CXXC motif in NfuA on protein/cofactor structure. This variant has been reported in human patients and direct measurement of protein-bound lipoic acid in individual tissues showed marked decreases. Comparative structures of the wt and variant NfuA could offer therapeutic value. Four proteins will be cloned and purified to study the LipA-NfuA interaction. Wt *Te* LipA and *Te* NfuA will be used to assess activity and crystallization propensity. *Te* NfuA G55C will serve as the G208C analog. A commercial synthetic construct was created by fusing the *Ec* NfuA N-terminal domain to the *Te* NfuA wt.

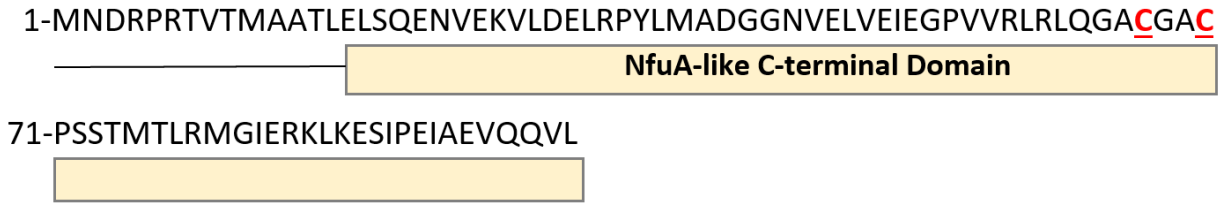

Figure 9. *Te* NfuA monomer sequence.

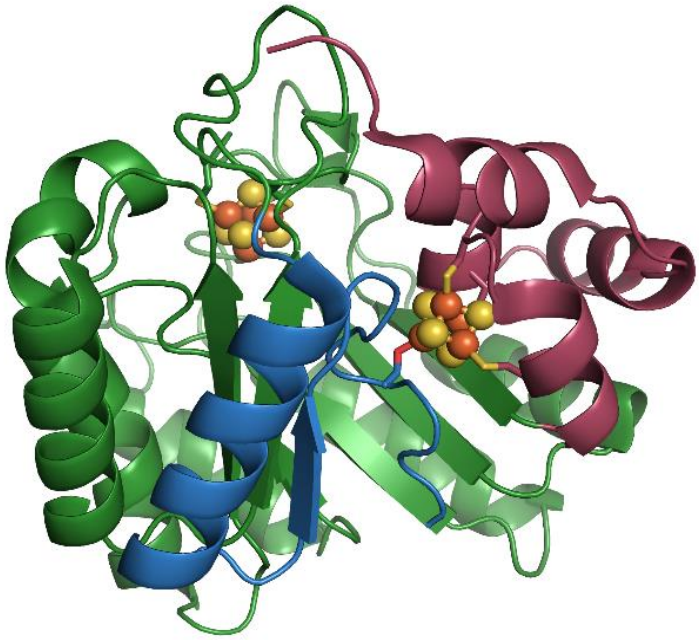

Figure 10. *Te LipA* crystal structure (1.6 Å resolution), including 2 $[4Fe\text{-}4S]^{2+}$ clusters at opposite ends of the TIM barrel. In addition to the three cysteine residue ligands, the auxiliary cluster is bound by a serine residue PDB accession code 4U0P. [13]

Chapter 2: *Te* LipA-*Te* NfuA Interaction

The work in this chapter aims to identify another system in which wild-type LipA and NfuA can execute multiple turnovers of lipoic acid. We found such a system in the *Te* LipA-NfuA pair sourced from a thermophilic bacterium. Identification of a functional LipA and NfuA with increased thermal stability could allow us to develop an ideal platform for distinguishing the exact mode of NfuA-mediated regeneration of LipA's auxiliary cluster.

The aforementioned gene constructs were purchased commercially from Invitrogen and amplified using the polymerase chain reaction (PCR), restriction digestion, bacterial transformation, plasmid purification, bacterial expression, and harvest. The proteins were soluble and successfully purified (Appendix B) with full occupancy of iron-sulfur clusters. Iron-sulfur cluster content was characterized using UV-vis spectroscopy and inductively coupled plasma - atomic emission spectroscopy (ICP-AES) analysis. Through activity assays, we showed that *Te* NfuA-LipA is the first biochemically characterized lipoic acid biosynthesis system identified to date in which an NfuA lacking the A-type N-terminal domain facilitates multi-turnover activity in LipA. And it is the second system after *Ec* NfuA-LipA to exhibit multiple turnovers. Our Se-labeled NfuA activity assay showed that NfuA enables incorporation of additional selenium into the lipoic acid product. However, selenium labeling of the auxiliary cluster slows down catalysis, hindering subsequent cluster transfers from NfuA to LipA. To determine the mechanism of LipA auxiliary cluster regeneration by NfuA in the *Te* system, we propose activity assays using ^{34}S *Te* NfuA wt and Se-labeled *Te* NfuA wt to track selenium cluster transfer from NfuA to LipA using X-ray crystallography.

2.1 Experimental Methods

Construction of expression vectors for LipA and NfuA proteins

The DNA sequences for the *Te* LipA, *Te* LipA NfuA wt, and *Ec* N-term NfuA-*Te* NfuA fusion were codon-optimized for expression in *E. coli* (Appendix A) and synthesized in a generic vector, PCR was used to amplify specific fragments of DNA using compatible forward and reverse primers in order to obtain sufficient amounts of the genes encoding *Te* LipA and NfuA to clone into an appropriate overexpression vector. The primers in Appendix A were designed as complementary to the template DNA sequence, and each primer contained the sequence of a

specific restriction endonuclease cutting site for digestion. We used this process to clone each gene into a pET28a expression vector using *NdeI* and *XhoI* restriction sites (Invitrogen Gene Art Gene Synthesis, ThermoFisher). The DNA sequences for all cloned genes were verified by Sanger sequencing (Genomics Core Facility, the Pennsylvania State University).

Overexpression and purification of LipA and NfuA proteins

The overexpression constructs in pET28a confer kanamycin resistance to transformed cells and gene expression is modulated by the strong T7 promoter, allowed for overproduction of the respective LipA and NfuA gene products. A second plasmid, pDB1282, encodes the *isc* operon from *Azotobacter vinelandii.* This vector confers ampicillin resistance, making it compatible for coexpression along with the LipA and NfuA encoding plasmids. Both plasmids were cotransformed into the *E. coli* BL21(DE3) expression system. The transformants were plated on Luria-Bertani (LB) plates containing kanamycin (50 μg/mL) and ampicillin (100 μg/mL). A single colony was selected and used to inoculate a culture of LB medium containing the same concentration of the aforementioned antibiotics and grown overnight at 37 ºC at 250 rpm. Simultaneously, four 6 L flasks containing M9 minimal medium (Appendix C Table C1) were placed in a shaker overnight at 37 ºC to warm the culture medium. Prior to inoculation, the M9 minimal medium was supplemented with D-glucose as the carbon source and antibiotics. The cultures were incubated at 37 ºC shaking at 180 rpm. At an OD_{600}, ~0.3 0.2% (w/v) L-arabinose was added to induce pDB1282 expression. At an OD_{600} ~0.6-0.8, the flasks were placed in an ice bath for 30 minutes, $FeCl_3$ was added to a final concentration of 50 μM and the incubation temperature was adjusted to 18 °C. After being cooled down, overexpression was induced by addition of 200 μM isopropyl-β-D-thiogalactopyranoside (IPTG) overnight at 18 °C with shaking at 180 rpm. The following day, the bacterial cells were harvested by centrifugation at 7500*g* for 12 minutes and the resulting cell pellets were flash-frozen in liquid nitrogen.

Iron-sulfur cluster proteins can undergo oxidative damage in the presence of oxygen, presenting challenges in isolation of holoenzymes. For this reason, all NfuA and LipA proteins were purified and characterized anaerobically. LipA is also sensitive to repeated freeze–thaw cycles. Purifications of this enzyme were therefore completed without interruption using chilled buffers, and the resulting pure proteins were stored in small aliquots to minimize damage. The general procedure for isolating oxygen-sensitive iron-sulfur-cluster-containing proteins has been previously described in detail.[38]

The cell pellets were resuspended in lysis buffer (Appendix C, Table C2) supplemented with lysozyme (1 mg/mL), DNase I (0.1 mg/mL), and PMSF (45 μg/mL). Once the solution was homogenized, the sonication cup was placed in an ice-water bath on a stir plate and the cells were lysed by sonic disruption in 10 second intervals for 50 minutes at 50% amplitude. Following sonication, the lysate was transferred to an autoclaved centrifuge tube and sealed with vinyl table to avoid oxygen contamination. The tube was removed from the anaerobic glove box and centrifuged at 22,000*g* for 70 minutes at 4 °C. Simultaneously, affinity resin was regenerated using ethylenediaminetetraacetic acid (EDTA) and $CoCl_2$ hexahydrate and equilibrated using a chilled lysis buffer. After equilibration, the supernatant was loaded onto the column and a flowthrough sample was collected. The column was washed with chilled wash buffer to remove unbound and nonspecifically bound proteins. The desired protein was eluted using chilled elution buffer. Collection started when the dark brown colored band began to elute and stopped once the color of the eluate returned to clear. The protein was concentrated using an Amicon® Ultra Centrifugal Filter. Once the protein was concentrated to ~2.5 mL, it was exchanged into a chilled gel filtration buffer using a PD-10 column. Concentrated protein was injected onto a HiLoad 16/600 Superdex 200 (S200) gel filtration column connected to an AKTA Pure FPLC system (GE Healthcare) Protein containing fractions were concentrated, flash-frozen in liquid N_2, and stored at -80 ºC for future studies. Protein concentrations were determined via the Bradford method using bovine serum albumin as a standard.[4]

Activity Assays

Reactions were performed in a Coy vinyl anaerobic chamber at room temperature. Reactions are typically prepared in a total volume of 200μL and contain the following: buffer (50 mM HEPES, pH 7.5, 200 mM KCl, 8% glycerol), 200 μM peptide substrate (Glu-Ser-Val-[N^6-octanoyl] Lys-Ala-Ala-Ser-Asp), 25 μM LipA, 0.5 μM S-adenosylhomocysteine (SAH) nucleosidase (to prevent product inhibition), and 1 mM SAM. An additional and identical reaction, but containing 500 μM NfuA, was also prepared. A 500 μL of a quench solution containing 100 mM H_2SO_4, 20 μM AtsA (peptide internal standard, Pro-Met-Ser-Ala-Pro-Ala-Arg-Ser-Met) and 4 mM TCEP was prepared and aliquoted into 8 microcentrifuge tubes. The reaction was initiated by adding 2 mM of the low potential reductant, sodium dithionite, and quenched by adding 20 μL of the reaction mix into 20 μL of quench solution at the appropriate time intervals. The reaction

tubes were centrifuged at 14000*g* x g for 30 min to remove precipitated protein. The supernatant from each time point sample was collected to quantify the lipoyl product by LC-MS.

Binding Assays

Qualitatively, molecular-sieve chromatography can be used to determine if in vitro mixtures of proteins coelute as a complex rather thanas individual components. A standard curve can be generated using a suite of standards in order to estimate the molecular weight of the complexes. The elution volume of Blue Dextran indicates the experimentally deter-mined void volume (V_0), and the elution volumes (V_e) of each of the additional standards, which will be used to generate a standard curve. Separately, samples of LipA and NfuA were loaded onto the column and eluted at a rate of 0.6 mL/min. Their elution volumes were recorded. A sample mixture containing both LipA and NfuA protein was incubated at room temperature for 5 minutes, loaded onto the column and eluted at 0.6 mL/min. Based on the observed peak in the chromatogram, protein containing fractions were collected and their elution volumes recorded. The fractions corresponding to each protein peak were concentrated and analyzed by SDS-PAGE to confirm the identity of the protein in each fraction. The experimentally determined elution volume of each of the peaks in the chromatograms of each sample were divided by the void volume of the column (V_e/V_o). The linear equation from the standard curve was used to solve for the logarithmic molecular weight of the individual proteins and the protein complexes.

2.2 Results and Discussion

Activity Assays of Te LipA with Te NfuA and the Ec N-term/Te NfuA fusion

All proteins were successfully purified with full iron-sulfur cluster occupancy (Appendix B). To ensure full reconstitution of cofactors, all purified protein samples were chemically treated with iron (III) chloride and sodium sulfide before they were subjected to size exclusion chromatography (SEC). Selenium labeled *Te* NfuA was generated by expressing *Te* NfuA wt apo and chemically reconstituting with iron (III) chloride and sodium selenite dissolved in dithiothreitol. SEC analysis reveal that *Te* LipA wt and *Te* LipA S283C eluted as monomers. *Te* NfuA eluted as a monomer and *Ec* N-term/*Te* NfuA's retention volume was between a monomer and a dimer (Figure 15, 16). NfuA is hypothesized to form a homodimer with a [4Fe-4S] cluster at the dimeric interface.[22] The oligomeric state of NfuA will be explored in the future with other techniques such as dynamic light scattering. The UV-vis spectrum of *Te* LipA, *Te* LipA S283C,

Te NfuA and *Ec* N-term/*Te* NfuA each showed a pronounced absorption shoulder at 400 nm which is a distinctive characteristic of $[4Fe\text{-}4S]^{2+}$ cluster containing proteins and gives a qualitative estimated of cluster occupancy (Appendices B7, B7, B8, and B6 respectively).[22] ICP-AES analysis showed *Te* LipA wt had 5.77 irons/protein (Appendix B7), *Te* LipA S283C had 6.76 irons/protein (Appendix B7), *Te* NfuA wt had 1.32 irons/monomer (Appendix B8) and *Ec* N-term/*Te* NfuA had 0.96 irons/protein (Appendix B6).

Our first experimental objective was to establish that *Te* LipA and NfuA were capable of multi-turnover activity. Mass spectrometry analysis of enzyme activity shows that *Te* LipA produces lipoic acid (996.5 m/z) (Figure 11). The magnitude of lipoic acid formation (996.5 m/z) was greatest for *Te* LipA wt + *Te* NfuA wt (blue trace) with clear evidence of multiple turnovers, with approximately a four-fold increase in the amount of product obtained with *Te* LipA wt (red trace). Surprisingly, addition of the *Ec* N-term-Te NfuA fusion (green trace) rendered LipA less active than wt NfuA, producing, at maximum, a two-fold increase in the amount of product compared to that formed with *Te* LipA wt. From these results, we have shown that *Te* system is the first system in which an A-type N-terminal domain lacking NfuA is able to facilitate multi-turnover activity in its native LipA and the second system after *Ec* system to facilitate multi-turnover activity in general. The ability of the *Te* system to operate as a robust multi-turnver enzyme with a short NfuA is surprising because it has been shown that the A-type N-terminal domain in *Ec* NfuA is absolutely necessary for multi-turnover activity in *Ec* LipA.[23]

Another interesting observation from this activity assay was that the *Ec* N-term/*Te* NfuA fusion was less efficient than *Te* NfuA in facilitating multi-turnover activity in *Te* LipA. Previous studies with *S. aureus* NfuA, which lacks the N-terminal A-type domain as in *Te* NfuA, was shown to have no effect on the activity of *Ec* LipA. However, fusing the *Ec* NfuA N-terminal domain to the *S. aureus* NfuA facilitated multi-turnover activity in *Ec* LipA.[23] *Te* LipA has adapted to use an NfuA that lacks an N-terminal A-type domain for multi-turnover activity.

We mutated *Te* LipA's conserved S283 in the RSSY motif to a cysteine (black trace) and found that this variant fails to form significant amounts of product. In wt LipA, the serine coordinates the fourth iron in the auxiliary cluster. This more labile ligand likely enables auxiliary cluster disassembly necessary for sulfur donation to the substrate. We predict that mutating the weaker serine ligand to a cysteine strengthens the bond to the iron thereby perturbing the reaction

kinetics since this iron is ejected into the solution after C6 sulfur insertion in wt LipA. Analogous mutations in *Ec* and *Mt* LipA have similar effects on enzyme activity.

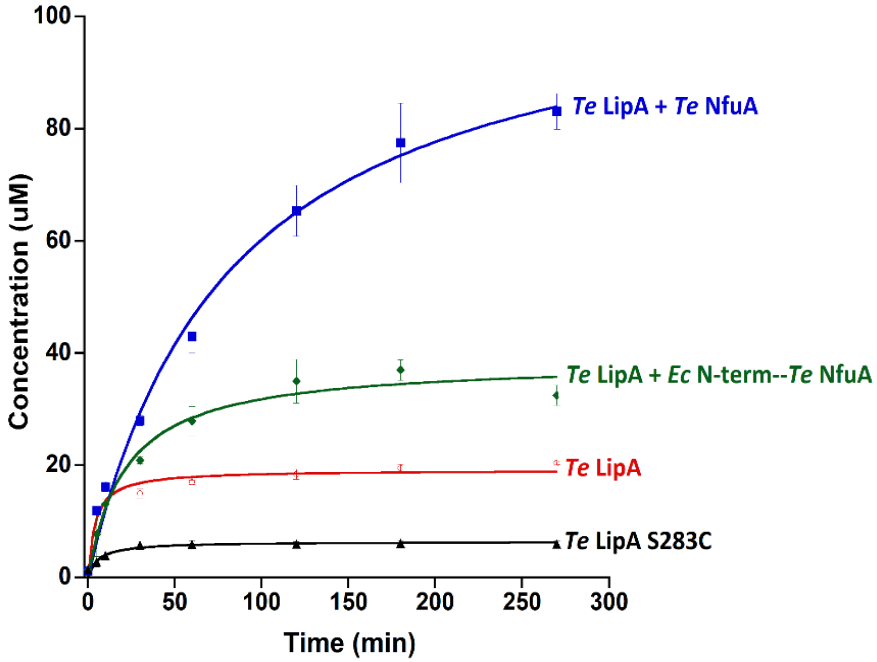

Figure 11. *Te* LipA lipoic acid formation (996.5 m/z). Each assay was performed using *Te* LipA or S283C (25 *μM)*, NfuA wt or *Ec* N-term-*Te* NfuA fusion (500 μM), substrate (200 μM), and SAM (1 mM) at room temperature under anaerobic conditions. Data points represent the average product concentration at each time point across three datasets. Error bars represent the standard deviation of these values. *Te* LipA + *Te* NfuA wt production formation (blue trace closed squares). *Te* LipA + *Ec* N-term-*Te* NfuA product formation (green trace closed diamonds). *Te* LipA wt product formation (red trace open circles). *Te* LipA S283C product formation (black trace closed triangles).

Monothiolated Intermediate Detection

We screened for the transient formation of the 964.5 m/z monothiolated intermediate using the same combination of proteins described in the previous section. Each sample displayed a unique pattern of intermediate formation. *Te* LipA alone and *Te* LipA with *Ec* N-term-*Te* NfuA exhibited an initial burst of the intermediate with a subsequent decline and plateau. *Te* LipA with *Ec* N-term-*Te* NfuA had a higher amount of intermediate formation compared to *Te* LipA alone which is correlated with the fact that *Ec* N-term-*Te* NfuA facilitates extra turnovers of lipoyl product. *Te* LipA with *Te* NfuA exhibited an initial burst of the intermediate with a subsequent decay and plateau. The plateaus occurs around 13 uM intermediate which is close to the amount of lipoyl product *Te* LipA alone makes directly, revealing a correlation with the amount active *Te*

LipA enzyme in this activity assay. This phenomenon has been observed in the *Ec* system. The other interesting finding is that *Te* LipA S283C, which barely makes any lipoyl product makes the same level of monothiolated intermediate when compared to *Te* LipA wt. This observation suggests that while the unique serine ligand is important for *Te* LipA catalysis, mutating it to a cysteine does not affect the first half of the reaction, namely C6 sulfur insertion. The role of this serine ligand will be studied extensively in the future via site directed mutagenesis. From the activity data, we can infer that the second sulfur insertion (second half of the reaction) occurs once a sizeable amount of the monothiolated intermediate is formed and C8 sulfur insertion is the rate limiting step.

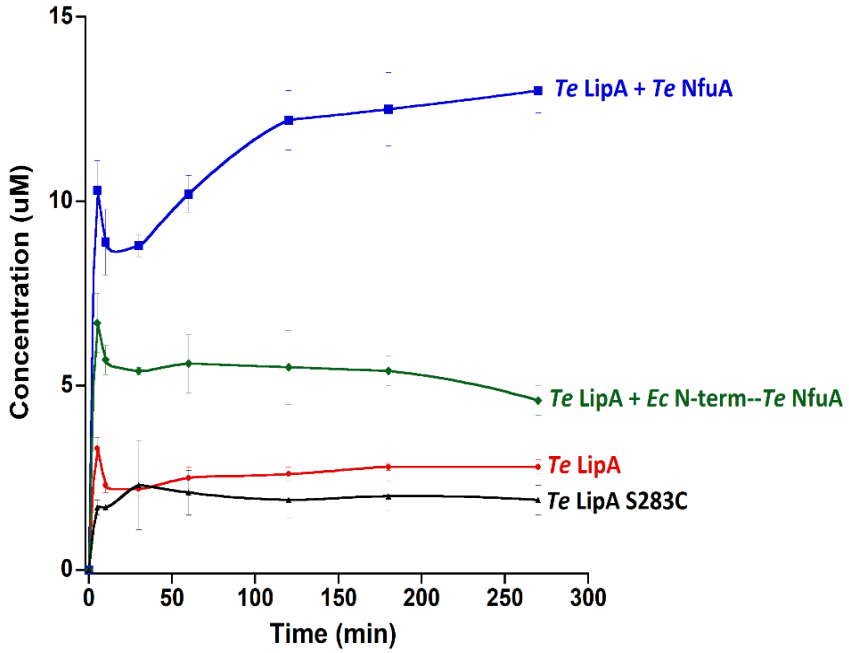

Figure 12. *Te* LipA monothiolated intermediate formation 964.5 m/z. Each assay was performed using Te LipA (25 *μM)*, NfuA wt or *Ec* N-term-*Te* NfuA fusion (500 μM), substrate 200μM, SAM (1 mM), and Citric Acid (1mM) at room temperature in anaerobic conditions. Error bars were generated using product concentrations across three datasets at corresponding times points. *Te* LipA + *Te* NfuA wt intermediate formation (blue trace closed squares). *Te* LipA + *Ec* N-term-*Te* NfuA intermediate formation (green trace closed diamonds). *Te* LipA wt intermediate formation (red trace closed circles). *Te* LipA S283C intermediate formation (black trace closed triangles)

Activity assays of Te LipA with Fe-Se Te NfuA

The goal of this experiment is to label NfuA with an iron-selenium cluster and track cluster transfer from NfuA to LipA. Ultimately, this approach could allow us to determine the identity of

the residual auxiliary cluster after a single turnover via X-ray crystallography. To perform the initial characterization of this system, we performed an activity assay with *Te* LipA and Fe-Se labeled *Te* NfuA to determine whether selenium-labeled *Te* NfuA is a compatible partner for LipA in the activity assay. Selenium-labeled *Te* NfuA was generated by reconstituting apo *Te* NfuA wt with iron and selenium. The reconstitution was successful and was confirmed by UV-vis spectroscopy (Appendix B8). The 280/400 nm ratio of Fe-Se *Te* NfuA was comparable to the sulfur-reconstituted *Te* NfuA. ICP-AES analysis of Fe-Se *Te* NfuA showed it had 1.22 iron/monomer and 0.101 selenium/monomer (Appendix B8). Activity assays were performed and reaction mixtures were screened for formation of the lipoic acid and seleno-lipoic acid products. Citric acid chelates free Fe^{2+} in solution, and its inclusion in the assay ensures that all product formation is due to direct cluster transfer from NfuA to LipA. Figure 13 shows that both *Te* LipA alone and *Te* LipA in the presence of Fe-Se *Te* NfuA produce one equivalent of lipoic acid. Screening for the seleno-lipoic acid formation, Figure 14, shows that Fe-Se *Te* NfuA promotes roughly an additional 0.75 equivalents of selenolipoic acid. This result was surprising because Fe-S NfuA (Figure 11) yields many more equivalents of product in that time frame. The difference in outcome suggests that the selenium-labeled auxiliary cluster slows down catalysis and perhaps blocks subsequent cluster transfers from NfuA to LipA. The overall finding in the *Te* system is subtly different from the previously characterized *Ec* system.[22] In the *Ec* system, *Ec* LipA in the presence of Fe-Se *Ec* NfuA produced <u>two</u> turnovers of lipoic acid and roughly one turnover of selenolipoic acid. *Ec* NfuA is able to help *Ec* LipA use the residual sulfurs in the auxiliary cluster for one extra turnover, thereby more efficiently using the entire auxiliary cluster for catalysis. In *Te* system, from our work, *Te* LipA cannot use the residual auxiliary cluster for an additional turnover of lipoic acid. This difference could be due to the lack of the N-terminal domain in *Te* NfuA and corresponding binding determinants for this domain in LipA.

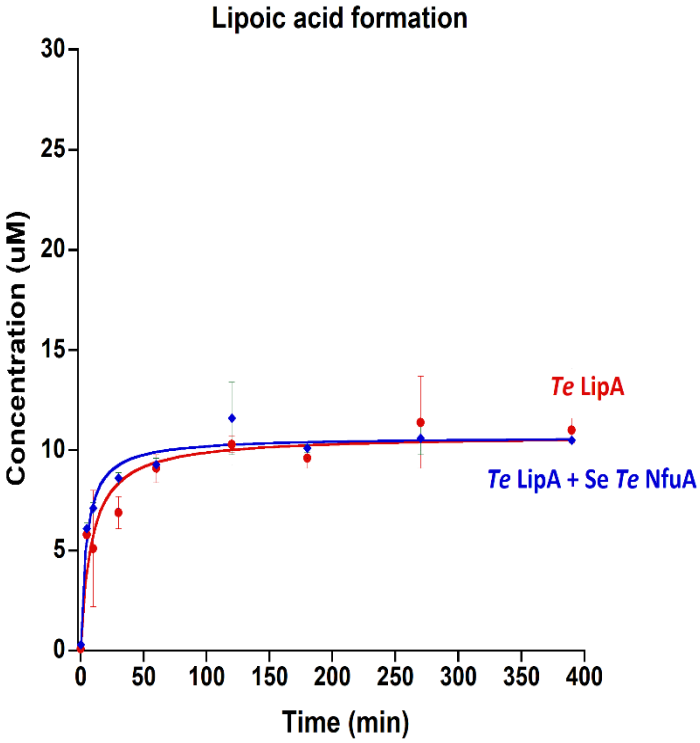

Figure 13. *Te* LipA activity assay screening for the thiolated product 996.5 m/z. Activity assays were performed using *Te* LipA (25 µM), Fe-Se Te NfuA (325 µM), substrate (200 µM), SAM (1 mM) and citric acid (1 mM). *Te* LipA (red trace closed circles), *Te* LipA + Fe-Se *Te* NfuA (blue trace closed squares).

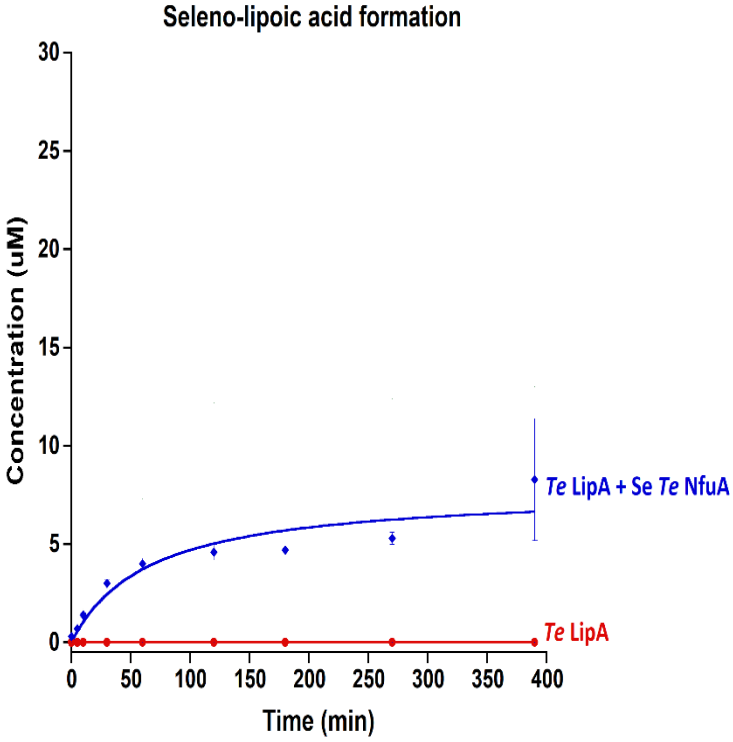

Figure 14. *Te* LipA activity assay screening for the selenated product 1090.5 m/z. Activity assays were performed using *Te* LipA (25 µM), Fe-Se *Te* NfuA (325 µM), substrate (200 µM), SAM (1 mM) and citric acid (1 mM). *Te* LipA (red trace closed circles) *Te* LipA + Fe-Se *Te* NfuA (blue trace closed squares).

Te LipA-NfuA Binding Assays

The goal of these experiments was to determine whether *Te* LipA- *Te* NfuA would form a stable complex and if it does, we can employ X-ray crystallography to elucidate the structure of this interaction. Analytical size exclusion column (SEC) chromatography was used to determine whether *Te* LipA wt and/or *Te* NfuA wt/*Ec* Nterm-*Te* NfuA form a complex. Protein content of each fraction was determined by SDS-PAGE. Fractions 22-26 correspond to *Te* LipA wt and fractions 22-28 correspond to *Te* NfuA. Despite an overlap in elution fractions, the gel shows individuals bands for the two proteins, suggesting they do not form a stable complex. If they instead formed a protein-protein complex, we would have observed a leftward shift in elution volume for the LipA peak, with bands for both proteins present on the gel. Previous studies in the *Ec* system have shown that *Ec* NfuA's N-terminal domain binds tightly with *Ec* LipA.[23] *Te* LipA and NfuA do not appear to bind tightly and this distinction, again, could be due to lack of an N-terminal A-domain in *Te* NfuA.

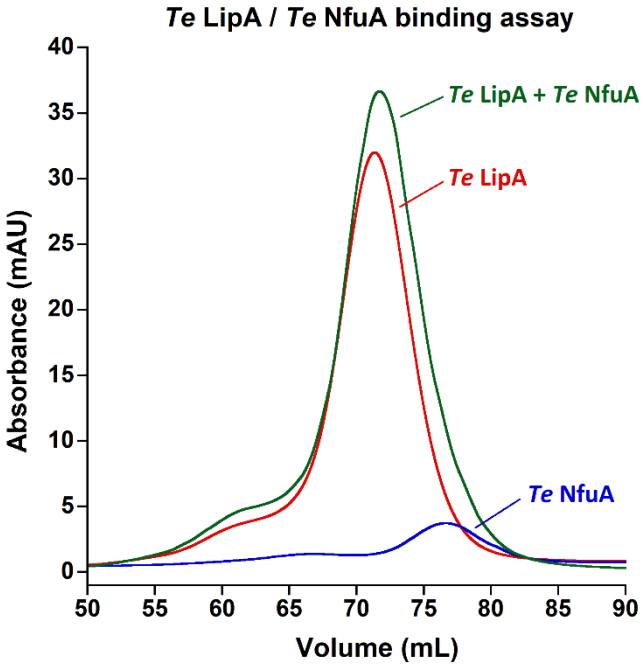

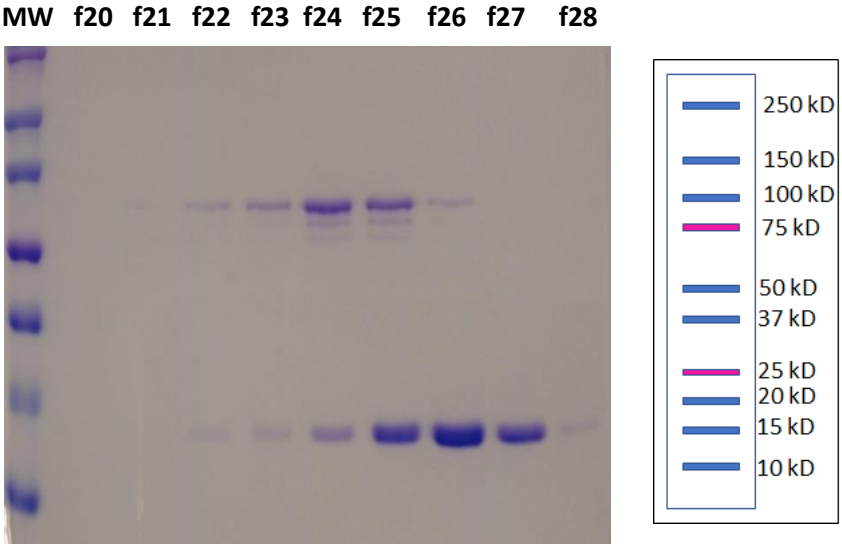

Figure 15. (Top) *Te* LipA/*Te* NfuA binding assay. (Bottom) Corresponding SDS-PAGE gel.
Te NfuA wt Theoretical MW: 12.00 kDa
Experimental MW: 11.85 kDa
Te LipA wt Theoretical MW: 32.55 kDa
Experimental MW: 18.46 kDa

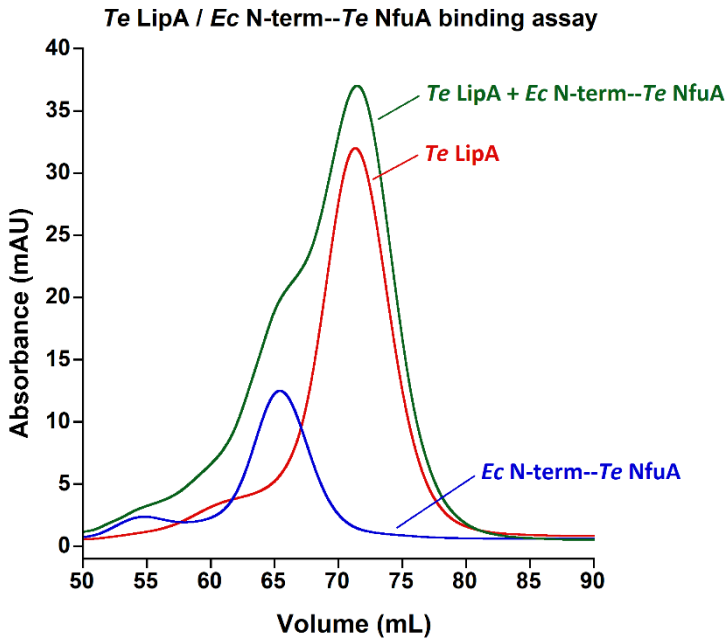

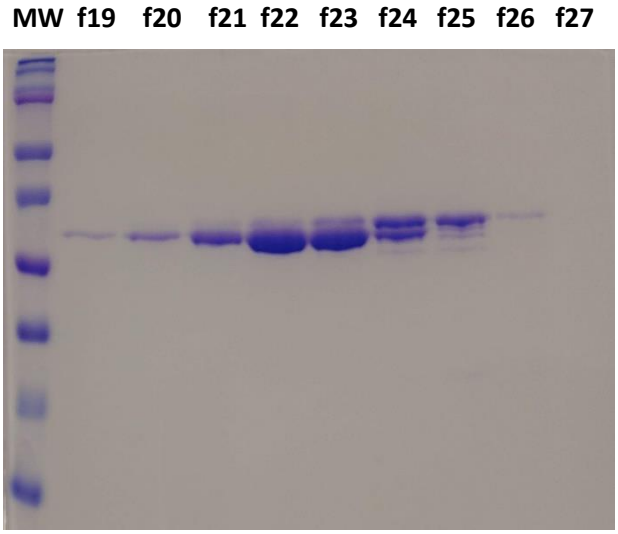

Figure 16. (Top) *Te* LipA/*Ec* Nterm-*Te* NfuA binding assay. (Bottom) Corresponding SDS-PAGE gel.
Te NfuA fusion Theoretical MW: 24.82 kDa
Experimental MW: 30.54 kDa
Te LipA wt Theoretical MW: 32.55 kDa
Experimental MW: 18.46 kDa

2.3 Conclusion and Future Directions

Conclusions

With *Te* LipA-NfuA system, we were able to identify the first system characterized to date in which a truncated NfuA facilitates optimal turnover rates with its native LipA. *Te* LipA, in the presence of Fe-Se *Te* NfuA, produces one equivalent of lipoic acid, suggesting that *Te* LipA is not using the residual auxiliary cluster most efficiently for an additional turnover of lipoic acid. Size-exclusion chromatography of the *Te* LipA-NfuA complex, and SDS-PAGE analysis of the protein-containing fractions, shows weak binding affinity between the two proteins. The property is also unique in contrast to *Ec* LipA and *Ec* NfuA, which bind tightly. These differences probably ultimately arise from the ways in which *Te* LipA has adapted to use a NfuA lacking the N-terminal A-type domain for multi-turnover activity

Future Directions

Now that we have established that NfuA promotes LipA's multiturnover activity in the *Te* system, we would next like to determine to the exact mode by which NfuA regenerates LipA's auxiliary cluster. We suspect two possible mechanisms after the first turnover: the hypothesized residual auxiliary [2Fe-2S] cluster of LipA is used in a second turnover with the octanoyl substrate, after which NfuA inserts a $[4Fe\text{-}4S]^{2+}$ cluster into the empty auxiliary site. Alternatively, the hypothesized residual auxiliary [2Fe-2S] cluster of LipA is ejected into the solution, after which NfuA inserts a $[4Fe\text{-}4S]^{2+}$ cluster into the empty auxiliary site. To distinguish between these two options, we will perform an activity assay with ^{34}S-reconstituted NfuA and measure the ratio of labeled/unlabeled sulfides in the lipoyl product for wt and variant enzymes. We will also continue our efforts to use selenium, a common surrogate for sulfur, in reconstituting NfuA to regenerate the auxiliary cluster in LipA. Selenium allows us to use x-ray crystallography to study the intermediate state of the reaction. We will then collect anomalous diffraction datasets at the Se x-ray absorption edge to track the location of Se in LipA crystals. This information could elucidate the mechanism of auxiliary cluster transfer and assembly. The proposed methods are diagramed in Figures 17 and 18 respectively.

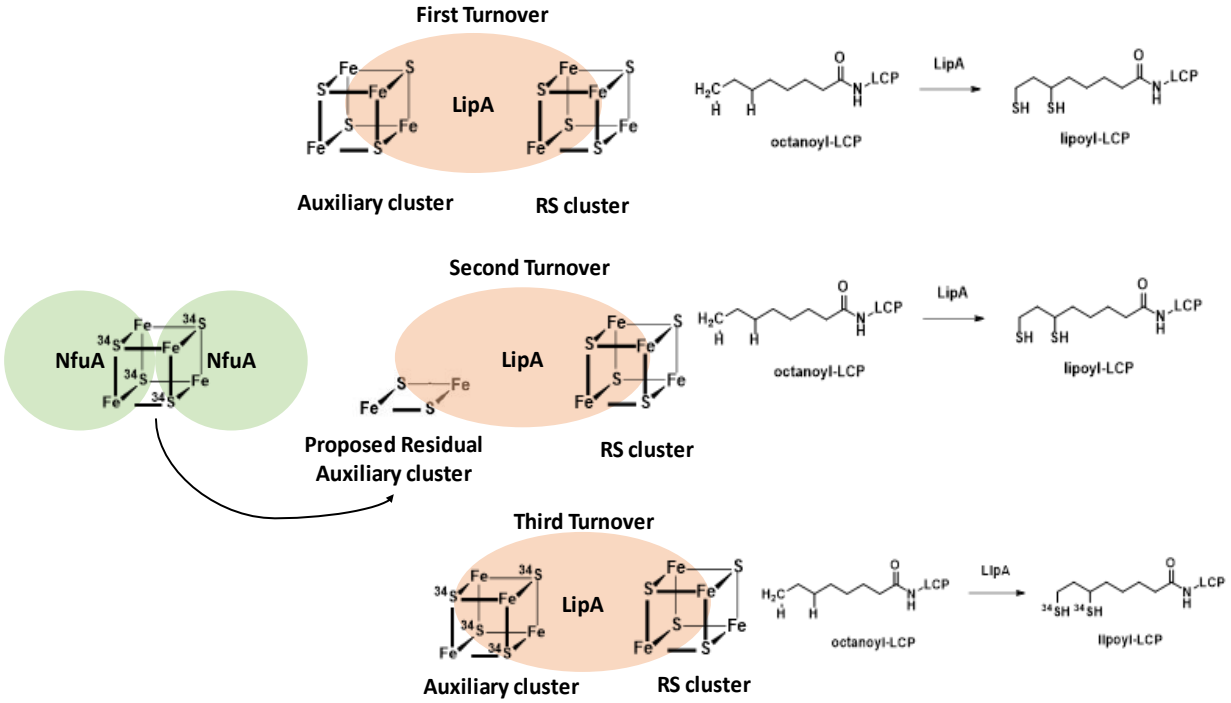

Figure 17. ^{34}S reconstituted *Te* NfuA and measure the ratio of labeled/unlabeled sulfides in the lipoyl product.

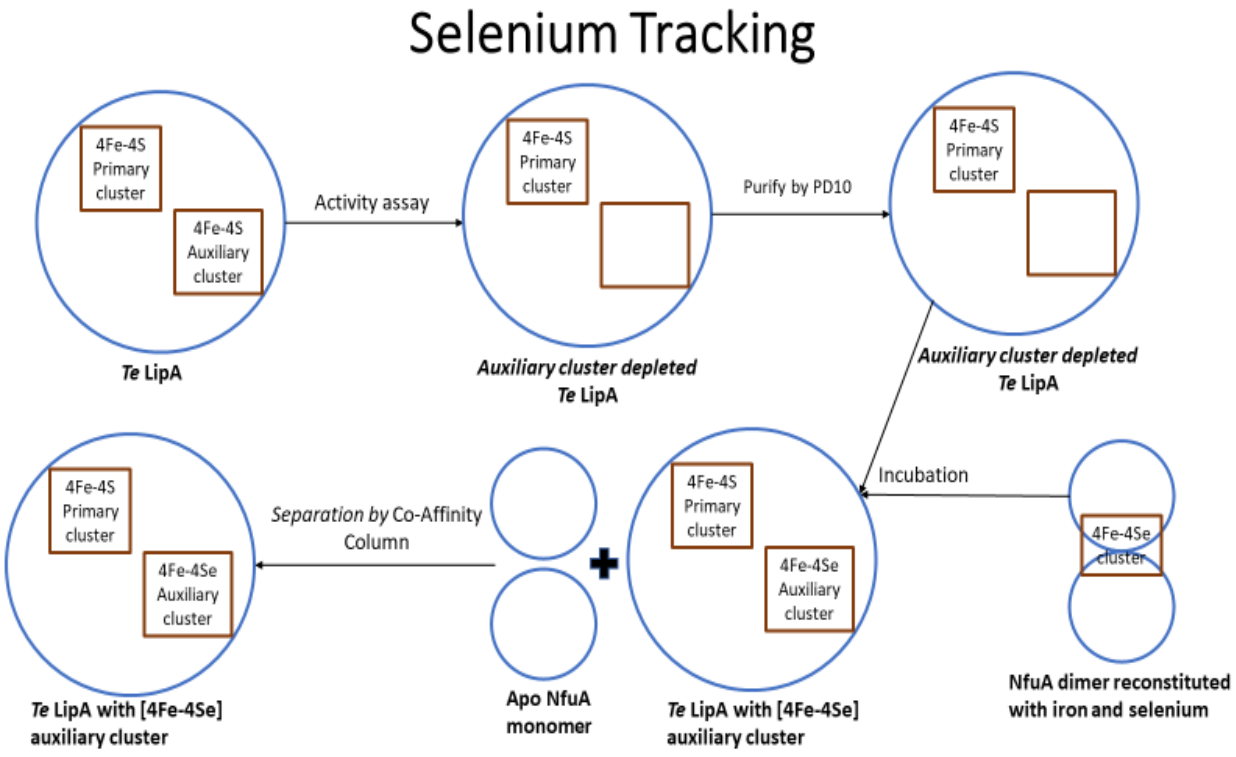

Figure 18. Se reconstituted *Te* NfuA for crystallographic characterization of *Te* LipA [4Fe-4S] auxiliary cluster regeneration.

Chapter 3: *Te* LipA-*Te* NfuA G55C Interaction

Human NFU1 consists of two domains, an N- and a C-terminal domain. The latter contains a highly conserved CXXC motif and is involved in the maturation of the iron-sulfur clusters on the [4Fe-4S] target proteins such as LipA.[29,40] Homologs of human NFU1 have been implicated in similar roles, involving both [2Fe-2S] and $[4Fe\text{-}4S]^{2+}$ cluster transfer, suggesting that both functionalities are possible and potentially physiologically relevant.[40] A G208C missense mutation in the protein close to the iron-sulfur (Fe/S) cluster binding motif alters the region around the cluster binding motif from GXCXXC to CXCXXC.[29,40] Studies have demonstrated that the mutation does not diminish the level of NFU1 expressed inside the cell but the identification of the global cellular effect of the NFU1 mutation shows marked decreases in protein-bound lipoic acid in individual tissues.[29] Despite the profound biological effects of this variant, we don't understand the influence of the mutation at the molecular level.[40] Analytical ultracentrifugation profiles for G208C NFU1 was monitored for sedimentation at 280 nm. Dimeric and higher order structures constituted 65.5% of the total protein species suggesting that the variant increases the propensity to oligomerize to impair downstream cluster trafficking.[40] Since alternative *in vivo* reconstitution pathways haven't been identified, loss of LipA activity is most likely due to greater protein oligomerization stemming from a minor structural change.

To understand the effects of this mutation on the structure and function of NfuA, we generated a *Te* NfuA G55C variant and analyzed its properties and interaction with *Te* LipA wt as it may offer insight into the requirement of for conserved glycine near the NfuA iron-sulfur cluster binding motif for functional LipA-NfuA interaction. One concern with the G→C variant is that it simply results in misfolded protein that you can't study biochemically. Given that NFU1 G208C is implicated in defective maturation of mitochondrial Fe-S proteins, we performed spectroscopic analysis, activity and binding assays to elucidate the variant's cluster assembly, function, and structure. We found that the G55C variant binds more iron per NfuA monomer, but it still promotes additional lipoic acid production compared to the activity of *Te* LipA alone. Binding assays also reveal separate elutions of Te LipA and Te NfuA G55C, suggesting weak binding, as found with wt NfuA. To further validate the oxidation state and nuclearity of the iron-sulfur cluster in G55C NfuA, we propose Mössbauer spectroscopic analysis in future work.

3.1 Experimental Methods

Te NfuA G55C variant was purified as described for wt NfuA in Chapter 2. The *Te* NfuA G55C variant was generated by site directed mutagenesis PCR by using pET28a *Te* NfuA wt as the template (Appendix A.4). The variant was successfully expressed and purified (Appendix B4) with the properties described below.

3.2 Results and Discussion

Prior to conducting any activity assays, we verified that introducing the G55C mutation didn't alter NfuA's 4Fe-4S cluster. UV-vis spectroscopy and ICP were used to determine the variant's iron content. Figure 19 shows an overlay of *Te* NfuA wt and *Te* NfuA G55C UV-Vis features. Both proteins share the characteristic 280 nm and 400 nm of other NfuA homologs. The absorption peak at 400 nm corresponds to iron-sulfur cluster absorption bands. Observation of a band at 400 nm in G55C NfuA indicates that this variant still contains NfuA's Fe-S center, however the variant has a more pronounced intensity. The 280:400 ratio for the wt is ~2 while for the variant it is ~1.4. This pattern suggests that the variant assembles an Fe-S cluster with a greater occupancy or different nuclearity than its wt counterpart. It is also possible that *Te* NfuA G55C possess a different quaternary structure, which could be investigated further by x-ray crystallography. An x-ray crystal structure of the variant protein could also shed light on the requirement for a glycine at that position for protein/cofactor stability.

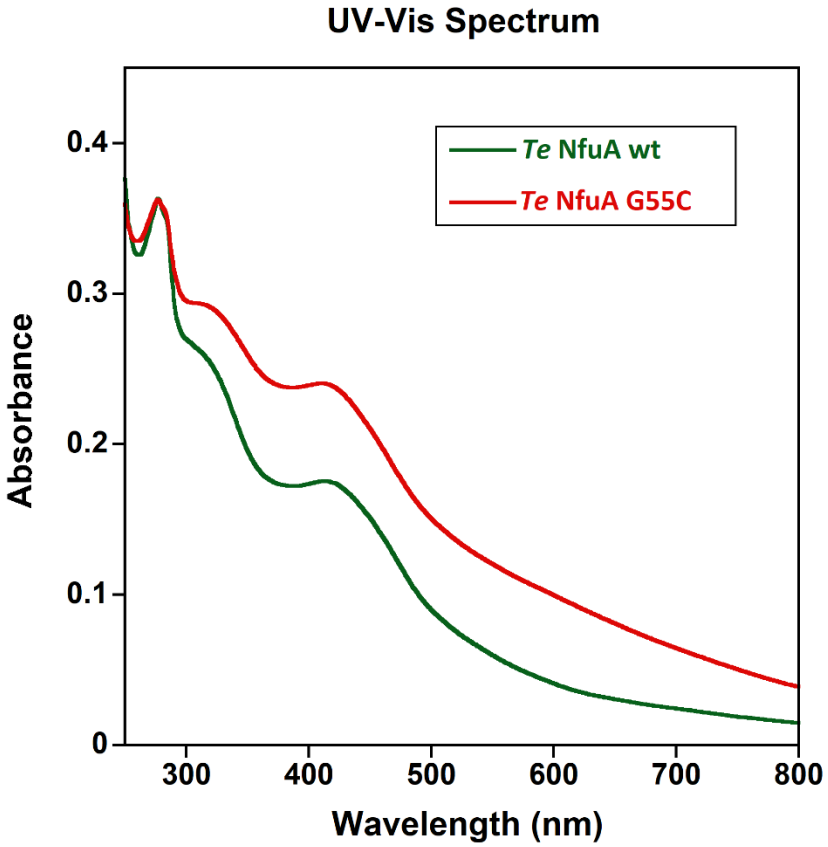

Figure 19. *Te* NfuA wt and G55C variant UV-vis spectra. ICP analysis reveals 2.29 Fe/monomer for *Te* NfuA G55C and 1.32 Fe/monomer for *Te* NfuA wt. UV-vis spectra were normalized at 276 nm to best illustrate differences around 400 nm.

Activity Assay: Te LipA with Te NfuA G55C

Figure 20 compares the activities of the variant and wt NfuA with LipA wt. *Te* LipA alone formed 3 µM lipoyl product. In the presence of *Te* NfuA wt, *Te* LipA formed 41 µM of lipoyl product, which corresponds to ~14 turnovers. In the presence of *Te* NfuA G55C, *Te* LipA showed 22 µM of lipoyl product which corresponds to ~7 extra turnovers. This result was surprising because the same mutation in human NFU1 leads to lethality. We expected *Te* NfuA G55C to show no enhancement of activity on *Te* LipA, or perhaps to even inhibit LipA activity entirely. Instead, our results show that *Te* NfuA G55C is still able to facilitate multi-turnover activity in *Te* LipA albeit at a slower rate than the wt NfuA. Product formation by *Te* NfuA G55C supplemented *Te* LipA was comparable to the levels observed with *Ec* N-term/*Te* NfuA fusion. This observation also supports the idea that the *Ec* NfuA's N-terminal domain has an inhibitory effect on *Te* NfuA wt activity. We note that these activity results were based on single assay. Additional experiments will need to be performed to validate our findings. In subsequent experiments, we also hope to

address the low levels of overall activity observed in this assay. Of the 30 μM of *Te* LipA wt used, only 3 μM product was observed. Because only 10% of the wt LipA enzyme fraction was active, we will repeat the activity assays with fresh preparations of protein.

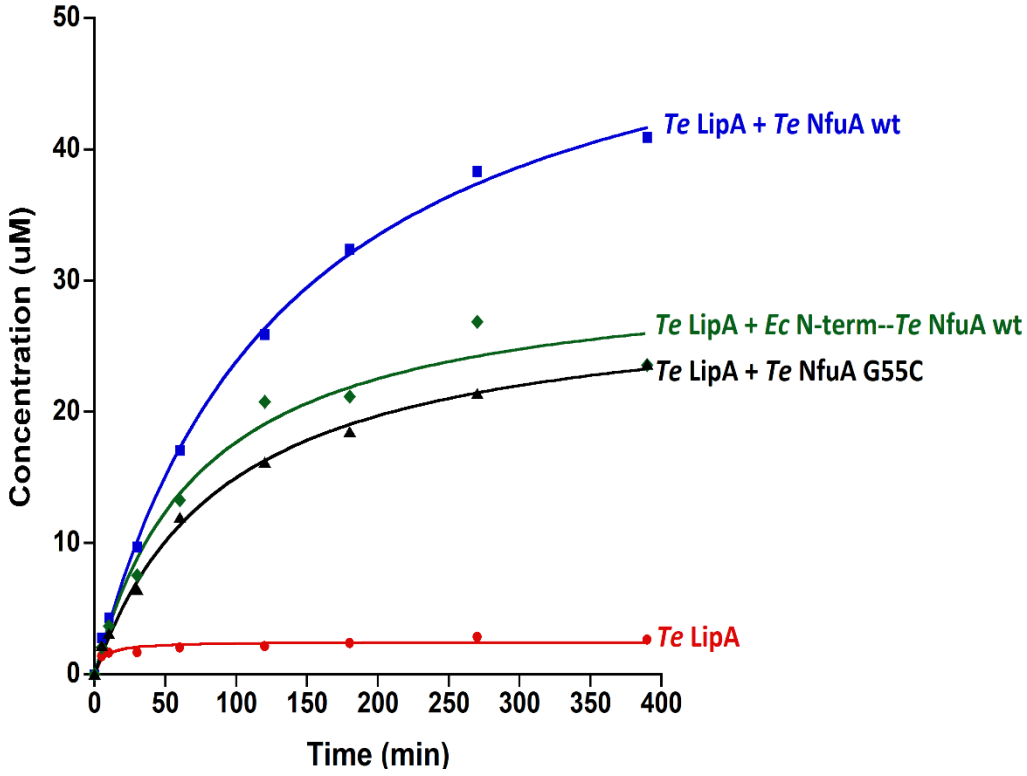

Figure 20. *Te* LipA activity assay with different NfuA constructs showing lipoyl product (996.5 m/z) formation. Each assay was performed using *Te* LipA (25 μM*)*, NfuA wt, *Ec* N-term-*Te* NfuA fusion, or *Te* NfuA G55C (500 μM), substrate (200 μM), and SAM (1 mM) at room temperature under anaerobic conditions. *Te* LipA + *Te* NfuA wt production formation (blue trace closed squares). *Te* LipA + *Ec* N-term-Te NfuA product formation (green trace closed diamonds). *Te* LipA wt product formation (red trace closed circles). *Te* LipA + *Te* NfuA G55C product formation (black trace closed triangles).

Te LipA-NfuA Binding Assays

Size-exclusion chromatography analysis of *Te* NfuA G55C and LipA shows no leftward shift in retention volume (Figure 21). We therefore conclude that no significant complex formation occurs between *Te* LipA wt and G55C. Interestingly the variant NfuA elutes at 65 mL (30.5 kDa) while the wt elutes at 77 mL (11.8 kDa) suggesting that the variant NfuA exists in a higher-order oligomeric structure (Figure 21). When the elution profiles of *Te* NfuA wt and G55C were superimposed upon each other, both *Te* NfuA wt and G55C have peaks at 65 mL and 77 mL, but

the intensities differ. We speculate that *Te* NfuA exists in a dynamic equilibrium between a monomer and a higher-order oligomer, such as a dimer or trimer. *Te* NfuA wt tends to mainly stay in the monomer form which elutes at 77 mL and *Te* NfuA G55C tends to stay in a higher oligomeric form which elutes at 65 mL.(Figure 22). The difference in the partition between different oligomeric forms could explain why *Te* LipA + G55C NfuA gives a reduced rate of lipoic acid product formation compared to *Te* LipA wt + *Te* NfuA wt. If human G208C NfuA exibits similar properties, this phenomenon could explain why the G→C mutation leads to the lethality *in vivo*.

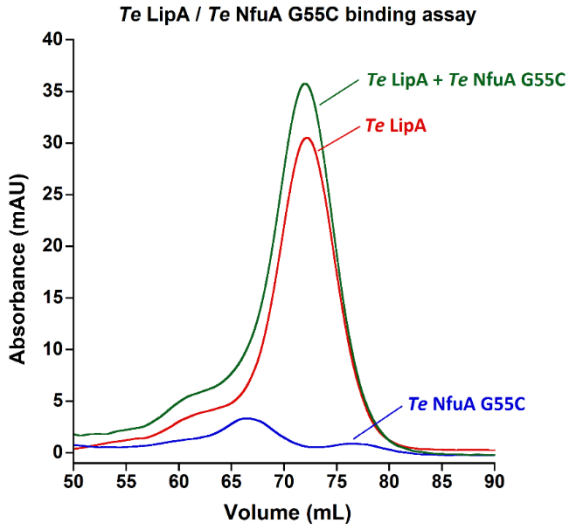

Figure 21. Elution profiles of *Te* LipA and *Te* NfuA G55C binding assay using wt and G55C Te NfuA. Retention volumes and calculated molecular weights on S200 column: Te NfuA wt 77 mL (11.8 kDa) and Te NfuA G55C 65 mL (30.5 kDa) compared to the theoretical 12.0 Kda)

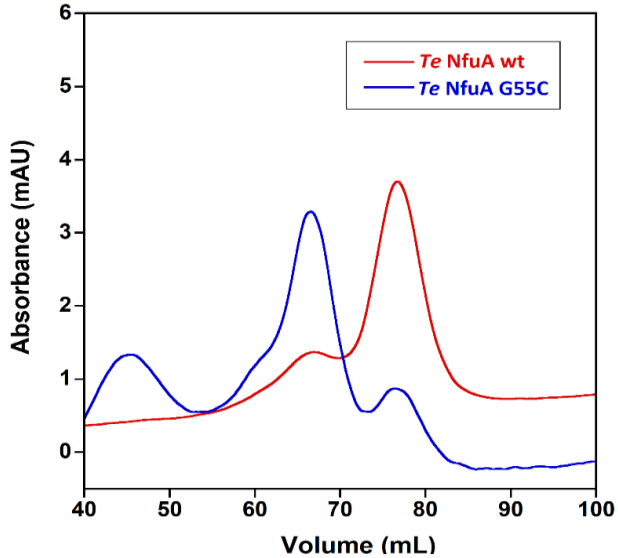

Figure 22. Superimposed elution profiles of *Te* NfuA wt and *Te* NfuA G55C.

3.3 Conclusions and Future Directions

Conclusions

Te NfuA G55C variant exists in a higher-order oligomeric structure with a stable [4Fe-4S]$^{2+}$ cluster. As in wt NfuA, the variant displays weak affinity towards *Te* LipA wt. The *Te* NfuA G55C variant also facilitates multi-turnover activity in *Te* LipA wt, albeit at a slower rate than *Te* NfuA wt.

Future Directions

In order to understand the form of iron bound to G55C NfuA and the basis for increased retention of metal, we will analyze this protein by Mössbauer spectroscopy. This method is particularly useful for this objective because adventitiously bound Fe will have a different characteristic spectrum than the Fe liganded by sulfurs in a [4Fe-4S] cluster, for example. Going forward, I will generate ^{57}Fe- labelled *Te* NfuA G55C to accurately deduce the iron-sulfur cluster composition using Mössbauer spectroscopy. The proposed method is diagrammed in Figure 23.

Mössbauer Spectroscopy of *Te* NfuA G55C

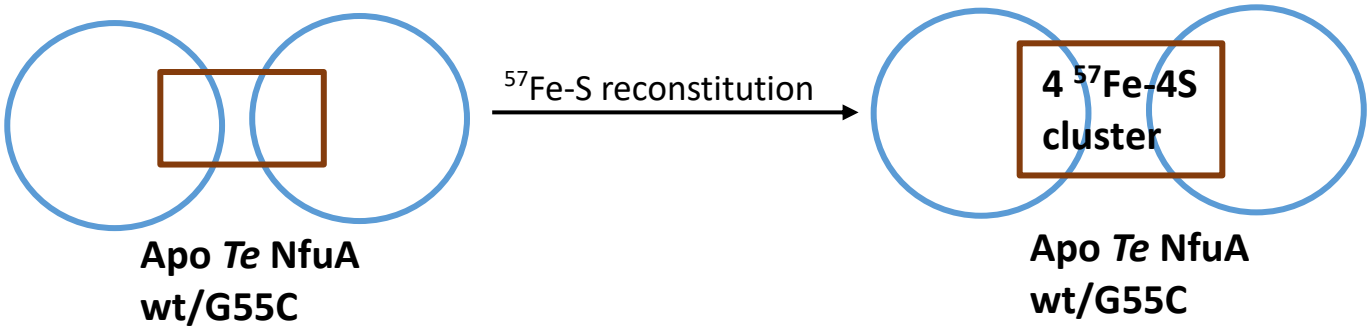

Figure 23. Proposed generation of ^{57}Fe labeled *Te* NfuA G55C. The protein will be flash frozen in liquid nitrogen and characterized by Mössbauer spectroscopy.

Appendix A

Codon-Optimized Gene Sequences of Protein Constructs

1. ***Te* LipA wt | Vector: pET26b**

CATATGGCACTGAGCCGTCCGCTGCCGAGCTGGCTGCGTAAACCGCTGGGTAAAGCAAGCGAAA
TTAGCACCGTTCAGCGTCTGGTTCGTCAGTATGGTATTCATACCATTTGTGAAGAAGGTCGTTG
TCCGAATCGTGGTGAATGTTATGGTCAGAAAACCGCAACCTTTCTGCTGCTGGGTCCGACCTGT
ACACGTGCATGTGCATTTTGTCAGGTTGAAAAAGGTCATGCACCGGCAGCAGTTGATCCGGAAG
AACCGACCAAAATTGCAGCAGCCGTTGCAACCCTGGGTCTGCGTTATGTTGTTCTGACCAGCGT
TGCACGTGATGATCTGCCGGATCAAGGTGCAGGTCAGTTTGTTGCAACCATGGCAGCAATTCGT
CAGCGTTGTCCGGGTACAGAAATTGAAGTTCTGAGTCCGGATTTTCGTATGGATCGTGGTCGTC
TGAGCCAGCGTGATTGTATTGCACAGATTGTTGCAGCACAGCCTGCATGCTATAATCATAATCT
GGAAACCGTTCGTCGTCTGCAGGGTCCTGTTCGTCGTGGTGCAACCTATGAAAGCAGCCTGCGT
GTTCTGGCAACCGTTAAAGAACTGAATCCGGATATTCCGACCAAATCAGGTCTGATGTTAGGTC
TGGGTGAAACCGAAGCAGAAATTATTGAAACCCTGAAAGATCTGCGTCGTGTTGGTTGTGATCG
TCTGACCCTGGGCCAGTATCTGCCTCCGAGCCTGAGCCATCTGCCGGTTGTGAAATATTGGACA
CCGGAAGAATTTAACACCCTGGGTAATATTGCCCGTGAACTGGGTTTTAGCCATGTTCGTAGCG
GTCCGCTGGTTCGTAGCAGCTATCATGCAGCAGAAGGTGGTCATCATCACCATCATCATTAACT
CGAG

Forward Primer
5’-TGTCCAGAGCTCCATATGGCACTGAGCCGTCCGCT-3’

Reverse Primer:
5’-GCTCCAGGTACCCTCGAGTTAATGATGATGGTGAT-3’

2. ***Te* NfuA wt | Vector: pET28a**

CATATGAATGATCGTCCGCGTACCGTTACCATGGCAGCAACCCTGGAACTGAGCCAAGAAAATGTTGAAA
AAGTTCTGGATGAACTGCGTCCGTATCTGATGGCAGATGGTGGTAATGTTGAACTGGTTGAAATTGAAGG
TCCGGTTGTTCGTCTGCGTCTGCAGGGTGCATGTGGTGCCTGTCCGAGCAGCACCATGACACTGCGTATG
GGTATTGAACGTAAACTGAAAGAAAGCATTCCGGAAATTGCAGAAGTTCAGCAGGTTCTGTAACTCGAG

Forward Primer:
5’-AAAAAAAAACATATGAATGATCGTCCGCGTACCGTTACC-3’

Reverse Primer:
5’-GCTCCAGGTACCCTCGAGTTACAGAACCTGCTGAAC-3’

3. *Ec* N-term NfuA-*Te* NfuA fusion | Vector: pET28a

CATATGATTCGCATTAGTGATGCAGCACAGGCACATTTTGCCAAACTGCTGGCAAATCAAGAAGAGGGCA
CCCAGATTCGTGTTTTTGTTATTAATCCGGGTACACCGAATGCAGAATGTGGTGTTAGCTATTGTCCGCC
TGATGCAGTTGAAGCAACCGATACCGCACTGAAATTTGATCTGCTGACCGCCTATGTTGATGAACTGAGC
GCACCGTATCTGGAAGATGCAGAAATTGATTTTGTTACCGATCAGCTGGGTTCACAGCTGACCCTGAAAG
CTCCGAATGCAAAAATGCGTAAAGTTGCAGATGATGCACCGCTGATGGAACGTGTTGAATATATGCTGCA
GAGCATGAATGATCGTCCGCGTACCGTTACCATGGCAGCAACCCTGGAACTGAGCCAAGAAAATGTTGAA
AAAGTTCTGGATGAACTGCGTCCGTATCTGATGGCAGATGGTGGTAATGTTGAACTGGTTGAAATTGAAG
GTCCGGTTGTTCGTCTGCGTCTGCAGGGTGCATGTGGTGCCTGTCCGAGCAGCACCATGACACTGCGTAT
GGGTATTGAACGTAAACTGAAAGAAAGCATTCCGGAAATTGCAGAAGTTCAGCAGGTTCTGTAACTCGAG
GGTACCTGGAGCACAAGACTGGCCTCATGGGCCTTCCGCTCACTGC

Forward Primer
5’-TGTCCAGAGCTCCATATGATTCGCATTAGTGATGCA-3’

Reverse Primer
5’-GCTCCAGGTACCCTCGAGTTACAGAACCTGCTGAAC-3’

4. *Te* NfuA G55C | Vector: pET28a

ATGAATGATCGTCCGCGTACCGTTACCATGGCAGCAACCCTGGAACTGAGCCAAGAAAATGTTGAAAAAG
TTCTGGATGAACTGCGTCCGTATCTGATGGCAGATGGTGGTAATGTTGAACTGGTTGAAATTGAAGGTCC
GGTTGTTCGTCTGCGTCTGCAGTGTGCATGTGGTGCCTGTCCGAGCAGCACCATGACACTGCGTATGGGT
ATTGAACGTAAACTGAAAGAAAGCATTCCGGAAATTGCAGAAGTTCAGCAGGTTCTGTAACTCGAG

Forward Primer G55C mutant:
5’-GTTCGTCTGCGTCTGCAGTGTGCATGTGGTGCCTGTCCG-3’

Reverse Primer G55C mutant:
5’-AACCGGACCTTCAATTTCAACCAGTTCAACATTACC-3’

Appendix B

Induction and Purification SDS-PAGE Gels and UV-VIS Spectra

1. pET26b *Te* LipA wt Induction and Purification Gels

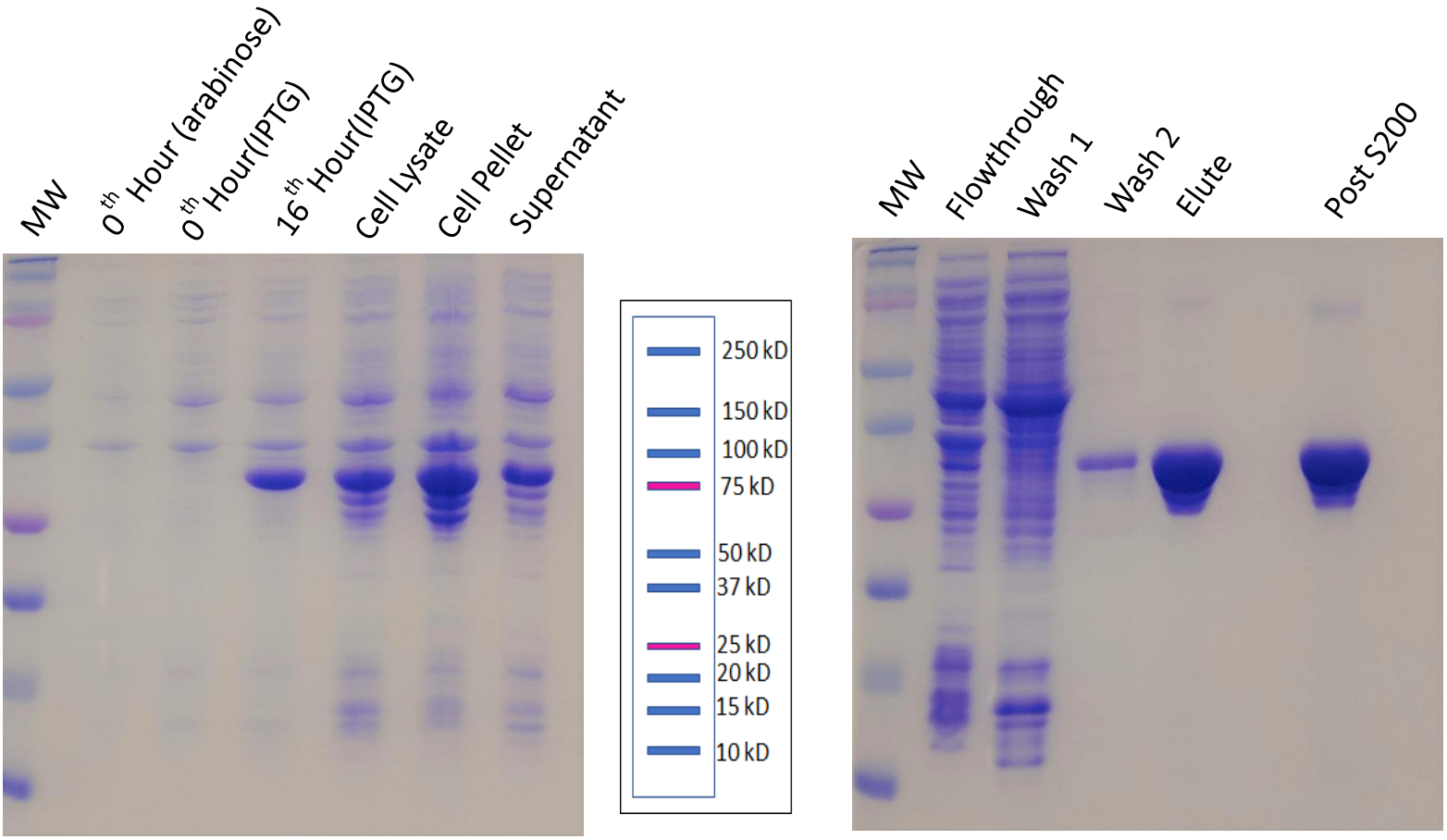

Appendix B1. Induction (Left) and Purification (Right) of pET28a *Te* LipA wt (32.55 kDa).

2. pET28a *Te* NfuA wt Induction and Purification Gels

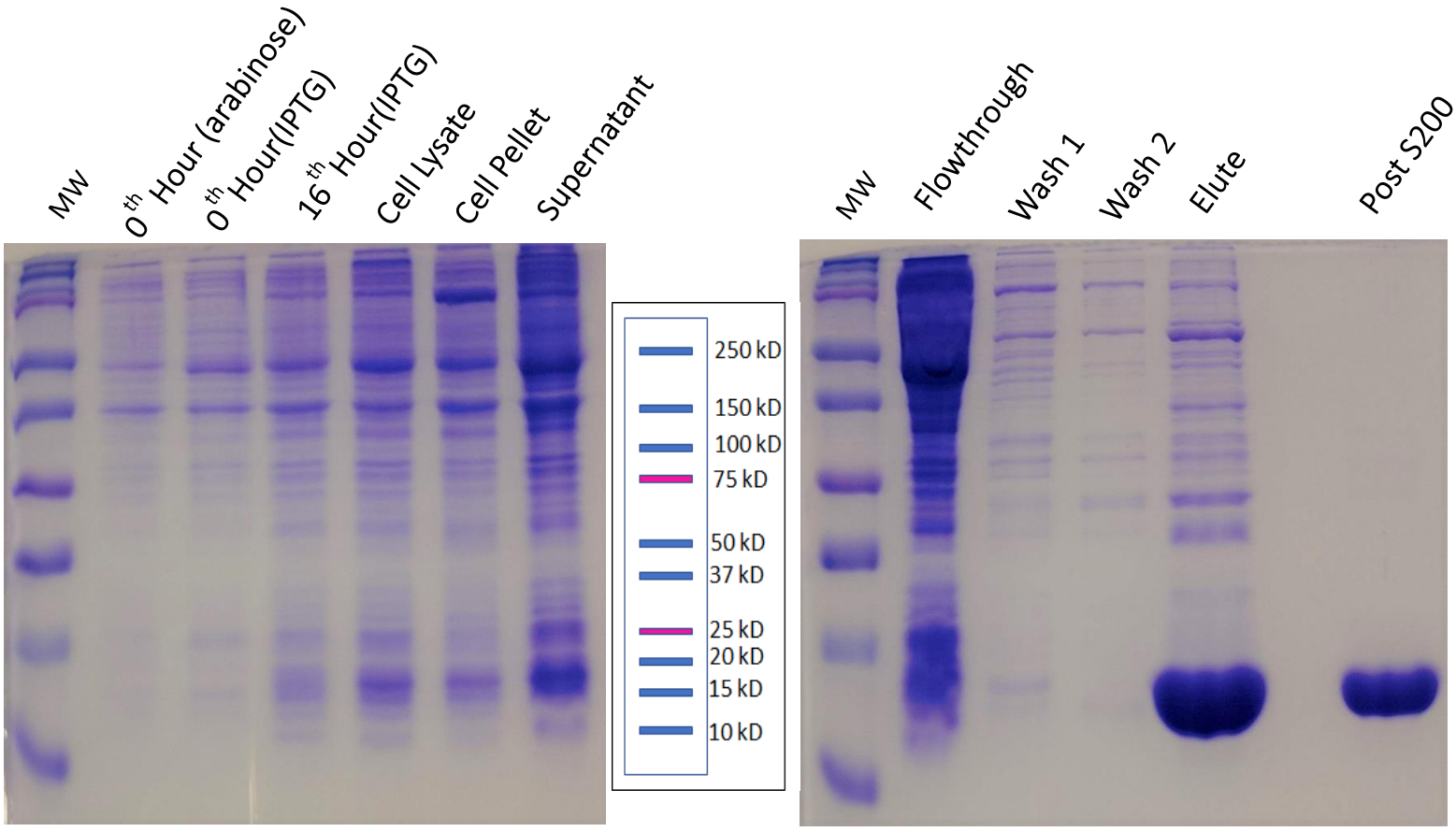

Appendix B2. Induction (Left) and Purification (Right) of pET26b *Te* NfuA wt (12.00 kDa).

pET28a *Ec* Nterm- *Te* NfuA wt fusion Induction and Purification

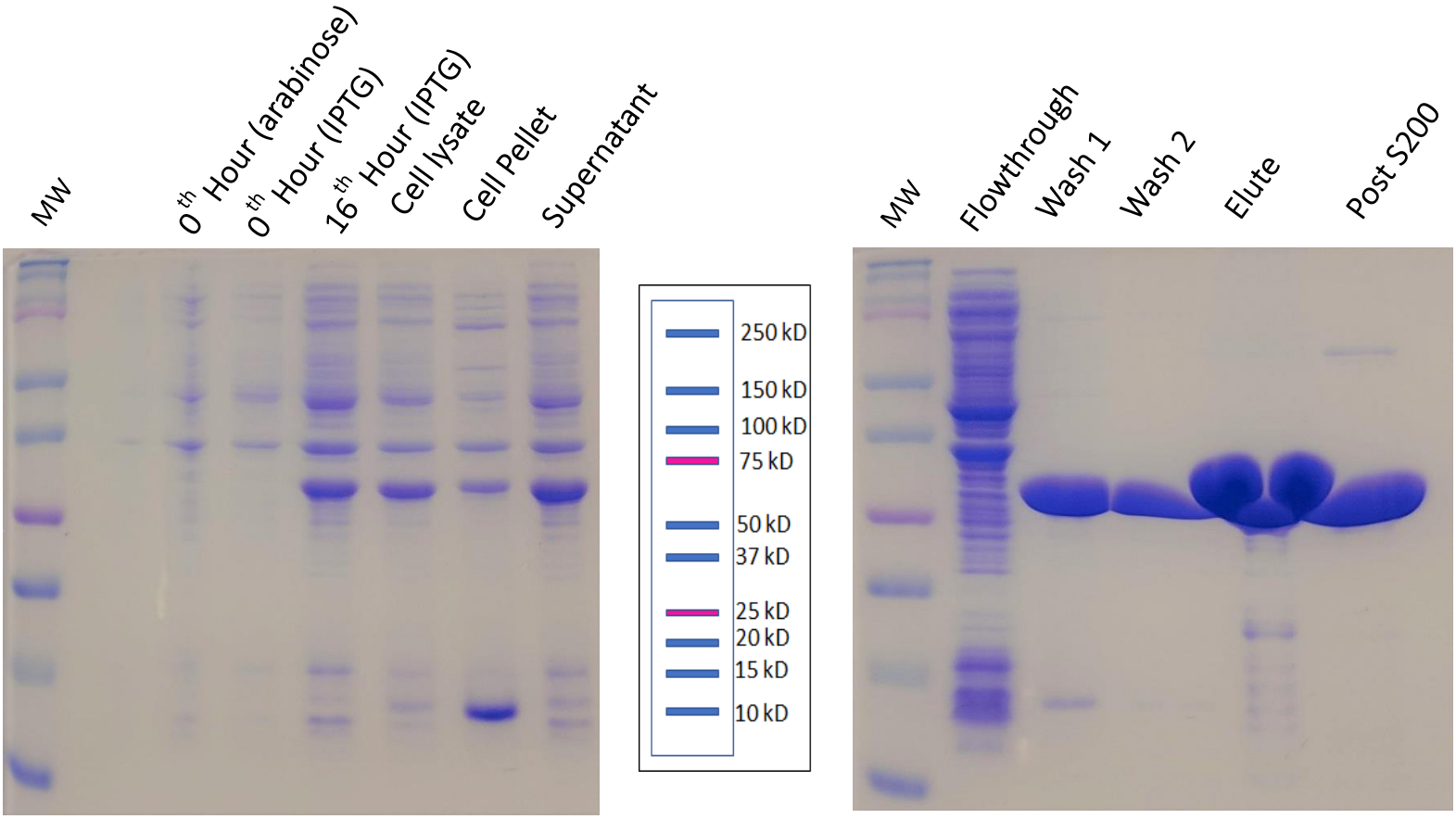

Appendix B3. Induction (Left) and Purification (Right) of pET28a *Ec* Nterm-*Te* NfuA wt (24.82 kDa).

2. pET28a *Te* NfuA G55C Induction and Purification

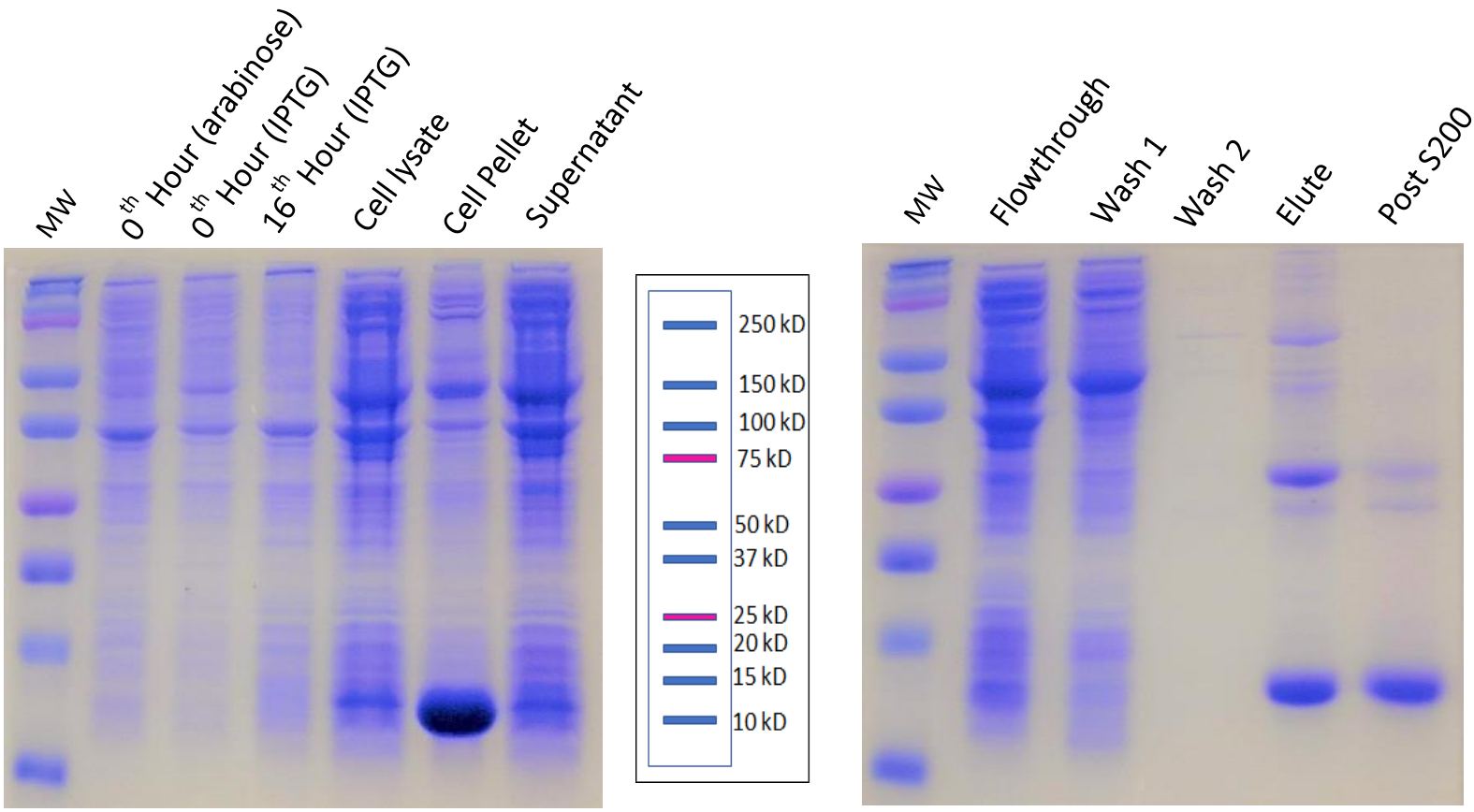

Appendix B4. Induction (Left) and Purification (Right) of pET28a *Te* NfuA G55C (Theoretical weight: 12.00 kDa).

3. pET28a *Te* LipA S283C Induction and Purification

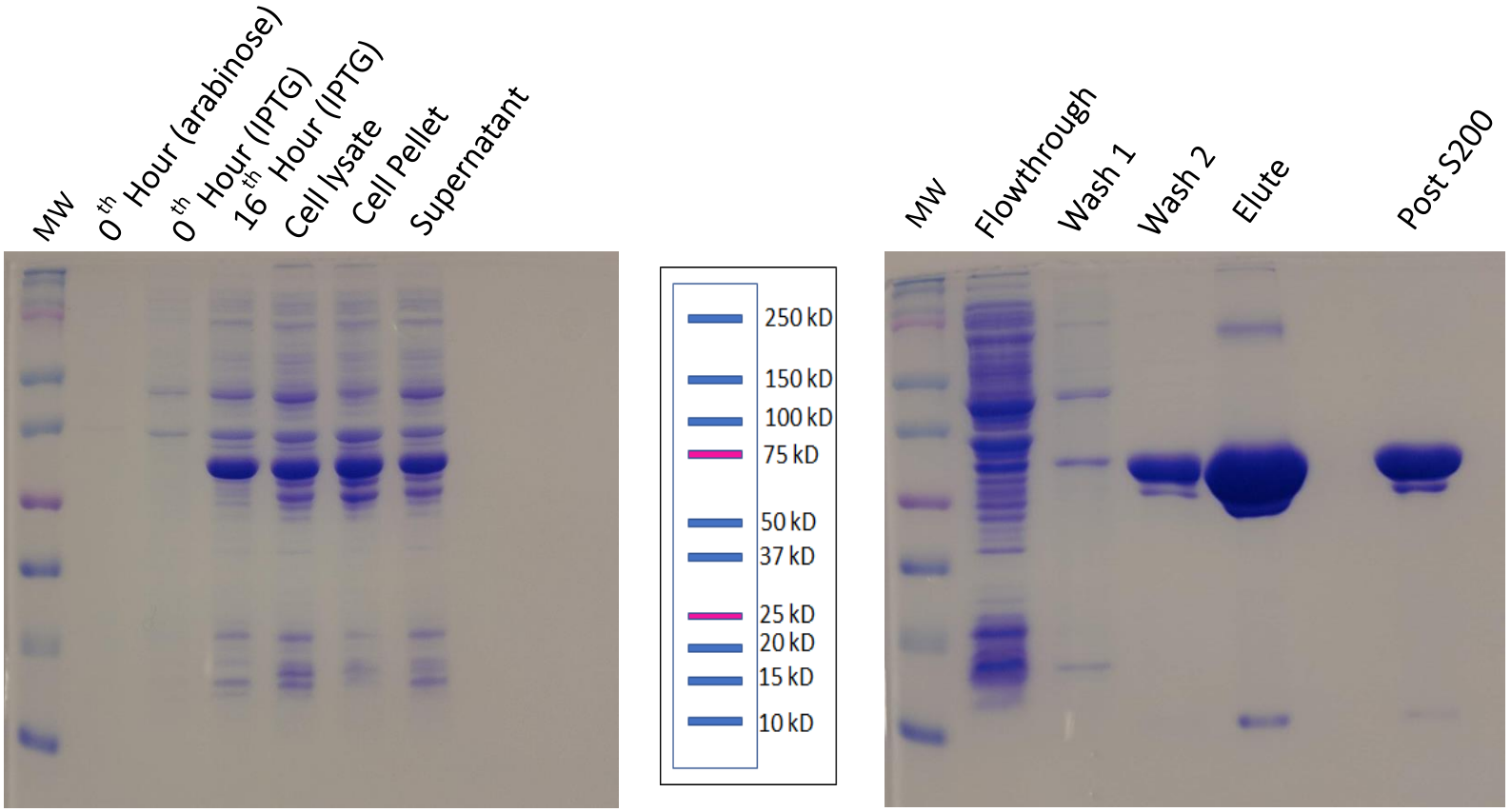

Appendix B5. Induction (Left) and Purification (Right) of pET28a *Te* LipA S283C (Theoretical weight: 32.55 kDa).

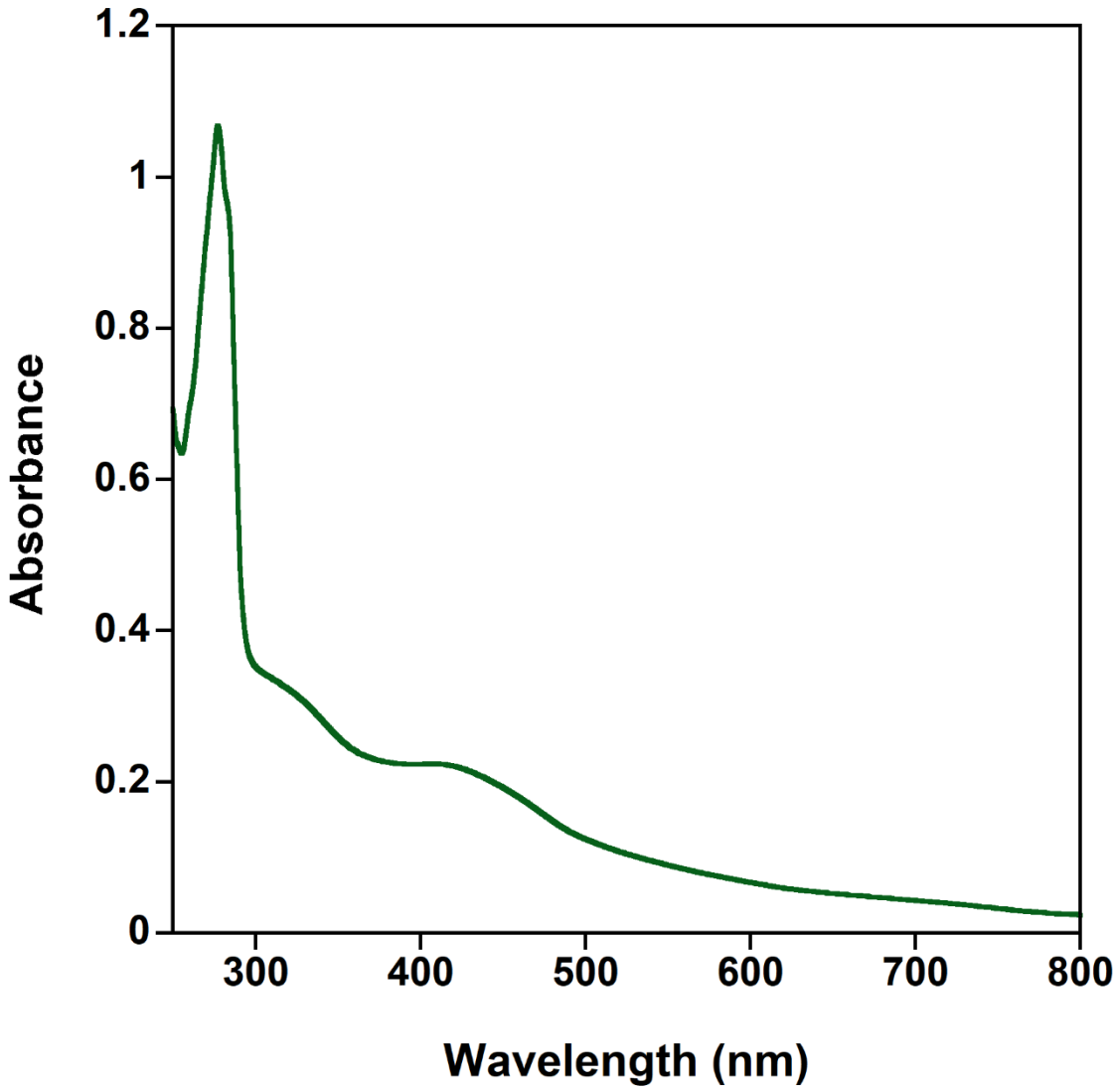

Appendix B6. *Ec*-Nterm *Te* NfuA wt UV-VIS spectrum.

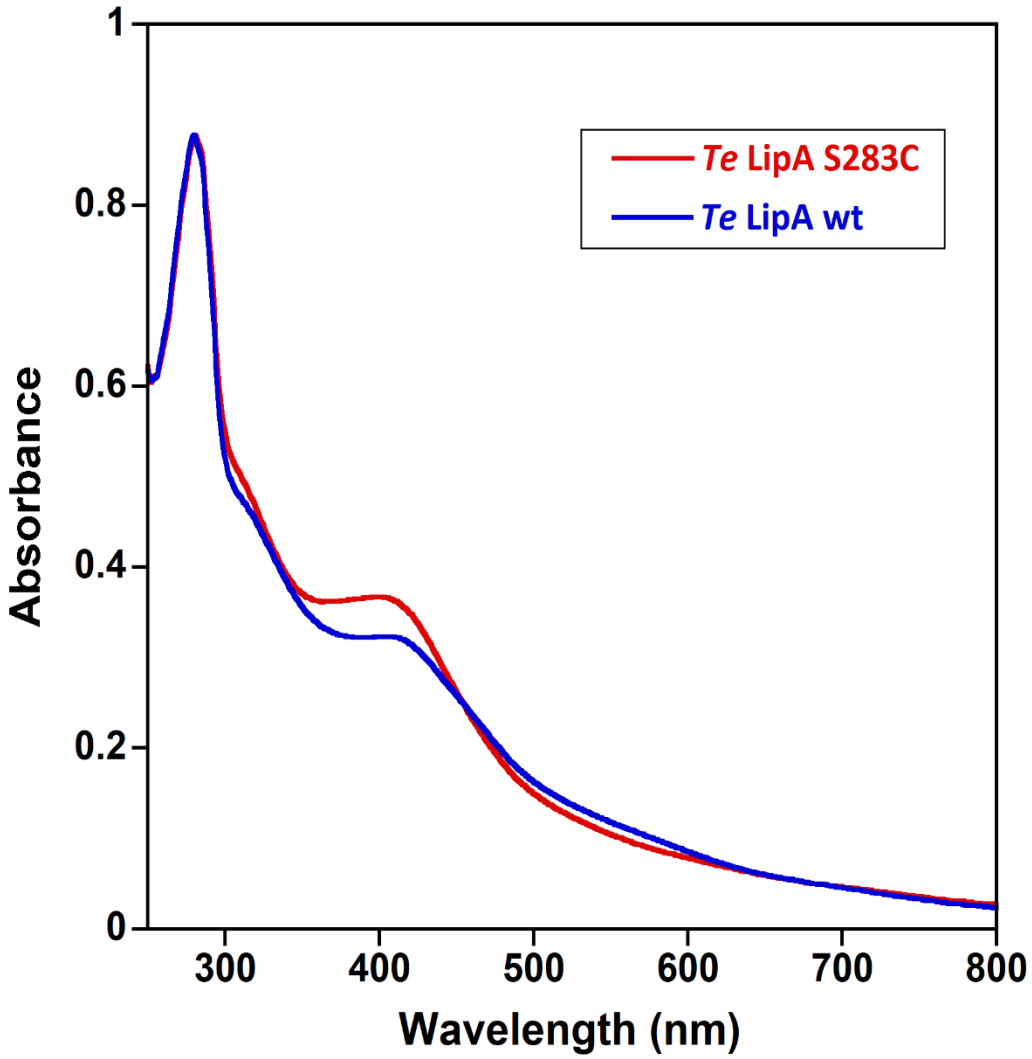

Appendix B7. Superimposed *Te* LipA wt and *Te* LipA S283C UV-vis spectrum (Normalised at 280 nm to see difference features at 400 nm). ICP-AES analysis reveals 5.77 Fe/protein for *Te* LipA wt and 6.76 Fe/monomer for *Te* LipA S283C

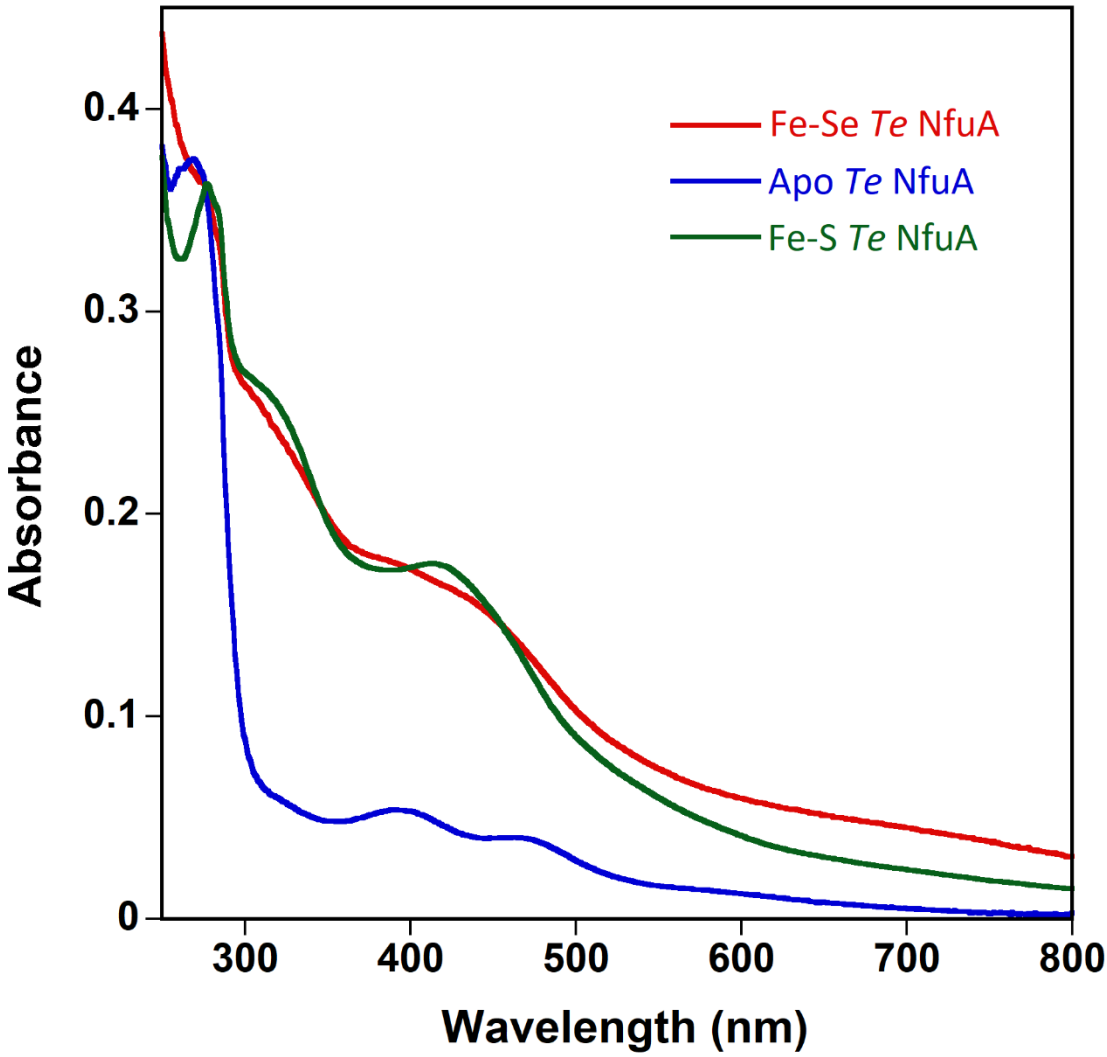

Figure B8. Se *Te* NfuA wt UV-VIS spectrum (red trace) superimposed with Apo *Te* NfuA (blue trace) and Fe-S *Te* NfuA (green trace). Normalized at 276 nm. Post Se-reconstitution of Apo *Te* NfuA a prominent shoulder at 400 nm, comparable to Fe-S *Te* NfuA, appears. ICP-AES analysis of Fe-Se *Te* NfuA showed it had 1.22 iron/monomer and 0.101 selenium/monomer.

Appendix C

Growth Media and Purification Buffers

Table C1. M9 Minimal Media			
20X M9 Salts (4L) pH 7.4		**Per 6L Flask**	
Na_2HPO_4	136 g	20X M9 Salts	200 mL
KH_2PO_4	60 g	ddH_2O	3700 mL
NaCl	10 g	AUTOCLAVE	
NH_4Cl	20 g	1M $MgSO_4$	8 mL
NaOH	6 g	1M $CaCl_2$	400 µL
KOH	7 g	20% D-Glucose	80 mL
ddH_2O (to 1 L)		100 mg/mL Ampicillin	4 mL
		50 mg/mL Kanamycin	4 mL

Table C2. Lysis Buffer			
Reagent	[I]	[F]	Volume
Hepes pH 7.5	1M	50 mM	12.5 mL
KCl	2.5 M	300 mM	30 mL
Imidazole	2M	20 mM	2.5 mL
BME	14.3M	10 mM	0.175 mL
H_20			197.5 mL
Total			250 mL

Table C3. Wash Buffer			
Reagent	[I]	[F]	Volume
Hepes pH 7.5	1M	50 mM	10 mL
KCl	2.5 M	300 mM	24 mL
Imidazole	2M	20 mM	2 mL
BME	14.3M	10 mM	0.14 mL
Glycerol	50%	10%	40 mL
H_20			115.36 mL
Total			200 mL

Table C4. Elution Buffer			
Reagent	[I]	[F]	Volume
Hepes pH 7.5	1 M	50 mM	12.5 mL
KCl	2.5 M	300 mM	30 mL
Imidazole	2 M	500 mM	62.5 mL
BME	14.3 M	10 mM	0.175 mL
Glycerol	50%	10%	50 mL
H_20		10%	87.33 mL
Total			250 mL

Table C5. Gel Filtration Buffer			
Reagent	[I]	[F]	Volume
Hepes pH 7.5	1 M	50 mM	12.5 mL
KCl	2.5 M	300 mM	30 mL
DTT	2 M	5 mM	5 mL
Glycerol	50%	15%	75 mL
H_20			120 mL
Total			250 mL

BIBLIOGRAPHY

1. Atta, M., et al., S-adenosylmethionine-dependent radical-based modification of biological macromolecules. *Curr. Opin. Struct. Biol*., 2010. **20**: p. 1–9.
2. Baldi, N., Dykstra, J. C., Luttik, M. A. H., Pabst, M., Wu, L., Benjamin, K. R., Vente, A., Pronk, J. T., & Mans, R. (2019). Functional expression of a bacterial α-ketoglutarate dehydrogenase in the cytosol of Saccharomyces cerevisiae. *Metabolic Engineering*, *56*, 190–197. https://doi.org/10.1016/j.ymben.2019.10.001
3. Bauerle, M.R., E.L. Schwalm, and S.J. Booker, Mechanistic diversity of radical S-adenosylmethionine (SAM)-dependent methylation. *J Biol Chem*, 2015. **290**(7): p. 3995-4002.
4. Bradford, M.M., A rapid and sensitive method for the quantitation of microgram quantities of protein utilizing the principle of protein-dye binding. *Anal Biochem*, 1976. **72**: p. 248-54.
5. Challand, M.R., R.C. Driesener, and P.L. Roach, Radical S-adenosylmethionine enzymes: mechanism, control and function. *Nat. Prod. Rep.*, 2011. **28**: p. 1696–1721.
6. Cicchillo, R. M., Lee, K., Baleanu-Gogonea, C., Nesbitt, N. M., Krebs, C., & Booker, S. J. (2004). Escherichia coli Lipoyl Synthase Binds Two Distinct [4Fe−4S] Clusters per Polypeptide†. *Biochemistry*, *43*(37), 11770-11781. doi:10.1021/bi0488505
7. Cicchillo, R. M., Iwig, D. F., Jones, A. D., Nesbitt, N. M., Baleanu-Gogonea, C., Souder, M. G., . . . Booker, S. J. (2004). Lipoyl Synthase Requires Two Equivalents of S-Adenosyl-l-methionine To Synthesize One Equivalent of Lipoic Acid†. *Biochemistry, 43*(21), 6378-6386. doi:10.1021/bi049528x
8. Cicchillo, R. M., & Booker, S. J. (2005). Mechanistic Investigations of Lipoic Acid Biosynthesis in Escherichia coli: Both Sulfur Atoms in Lipoic Acid are Contributed by the Same Lipoyl Synthase Polypeptide. *Journal of the American Chemical Society*, *127*(9), 2860-2861. doi:10.1021/ja042428u
9. Douglas, P., Kriek, M., Bryant, P., and Roach, P. L. (2006) Lipoyl synthase inserts sulfur atoms into an octanoyl substrate in a stepwise manner. Angew. *Chem., Int. Ed.* 45, 5197−5199
10. Frey, P. A., & Booker, S. J. (2001). Radical mechanisms of S-adenosylmethionine-dependent enzymes. Advances in Protein Chemistry,58,1–45.
11. Fugate, C.J. and J.T. Jarrett, Biotin synthase: Insights into radical-mediated carbon-sulfur bond formation. *Biochim. Biophys*. Acta, 2012.
12. Garcia-Serres, R., Clémancey, M., Latour, J., & Blondin, G. (2018). Correction to: Contribution of Mössbauer spectroscopy to the investigation of Fe/S biogenesis. *JBIC Journal of Biological Inorganic Chemistry*, *23*(4), 645-645. doi:10.1007/s00775-018-1572-6
13. Harmer, J., Hiscox, M., Dinis, P., Fox, S., Iliopoulos, A., Hussey, J., . . . Roach, P. (2014). Structures of lipoyl synthase reveal a compact active site for controlling sequential sulfur insertion reactions. *Biochemical Journal*, *464*(1), 123-133. doi:10.1042/bj20140895
14. Jordan, S. W., & Cronan, J. E. (2003). The Escherichia coli lipB Gene Encodes Lipoyl (Octanoyl)-Acyl Carrier Protein:Protein Transferase. *Journal of Bacteriology, 185*(5), 1582-1589. doi:10.1128/jb.185.5.1582-1589.2003

15. Jordan, S. W., and Cronan, J. E., Jr. (1997) A new metabolic link. The acyl carrier protein of lipid synthesis donates lipoic acid to the pyruvate dehydrogenase complex in Escherichia coli and mitochondria. *J. Biol. Chem. 272*, 17903−17906
16. Kikuchi, G., Motokawa, Y., Yoshida, T., & Hiraga, K. (2008). Glycine cleavage system: reaction mechanism, physiological significance, and hyperglycinemia. *Proceedings of the Japan Academy, Series B, 84*(7), 246–263. https://doi.org/10.2183/pjab.84.246
17. Lanz, N. D., Pandelia, M., Kakar, E. S., Lee, K., Krebs, C., & Booker, S. J. (2014). Evidence for a Catalytically and Kinetically Competent Enzyme–Substrate Cross-Linked Intermediate in Catalysis by Lipoyl Synthase. *Biochemistry, 53*(28), 4557-4572. doi:10.1021/bi500432r
18. Lanz, N. D., Rectenwald, J. M., Wang, B., Kakar, E. S., Laremore, T. N., Booker, S. J., & Silakov, A. (2015). Characterization of a Radical Intermediate in Lipoyl Cofactor Biosynthesis. *Journal of the American Chemical Society, 137*(41), 13216-13219. doi:10.1021/jacs.5b04387
19. Lanz, N. D., Lee, K., Horstmann, A. K., Pandelia, M., Cicchillo, R. M., Krebs, C., & Booker, S. J. (2016). Characterization of Lipoyl Synthase from Mycobacterium tuberculosis. *Biochemistry*, 1373-1384. doi:10.1021/acs.biochem.5b01216.s001
20. Lanz, N. D., & Booker, S. J. (2015). Auxiliary iron-sulfur cofactors in radical SAM enzymes. Biochimica et Biophysica Acta,1853(6), 1316–1334.
21. Marquet, A., B. Tse Sum Bui, and D. Florentin, Biosynthesis of biotin and lipoic acid. *Vitam. Horm*., 2001. **61**: p. 51-101.
22. Mccarthy, E. L., & Booker, S. J. (2017). Destruction and reformation of an iron-sulfur cluster during catalysis by lipoyl synthase. *Science, 358*(6361), 373-377. doi:10.1126/science.aan4574
23. Mccarthy, E. L., Rankin, A. N., Dill, Z. R., & Booker, S. J. (2018). The A-type domain in Escherichia coli NfuA is required for regenerating the auxiliary [4Fe–4S] cluster in Escherichia coli lipoyl synthase. *Journal of Biological Chemistry, 294*(5), 1609-1617. doi:10.1074/jbc.ra118.006171
24. McCarthy, E. L., & Booker, S. J. (2018). Biochemical Approaches for Understanding Iron-sulfur Cluster Regeneration in Escherichia coli Lipoyl Synthase during Catalysis. *Methods Enzymology, 606*, 217–239. https://doi.org/10.1016/bs.mie.2018.06.006
25. Mclaughlin, M. I., Lanz, N. D., Goldman, P. J., Lee, K., Booker, S. J., & Drennan, C. L. (2016). Crystallographic snapshots of sulfur insertion by lipoyl synthase. *Proceedings of the National Academy of Sciences, 113*(34), 9446-9450. doi:10.1073/pnas.1602486113
26. Miller, J. R., Busby, R. W., Jordan, S. W., Cheek, J., Henshaw, T. F., Ashley, G. W., Broderick, J. B., Cronan, J. E., Jr., and Marletta, M. A. (2000) Escherichia coli LipA is a lipoyl synthase: in vitro biosynthesis of lipoylated pyruvate dehydrogenase complex from octanoyl-acyl carrier protein. Biochemistry 39, 15166−15178.
27. Morris, T. W., Reed, K. E., and Cronan, J. E., Jr. (1994) Identification of the gene encoding lipoate-protein ligase A of Escherichia coli. Molecular cloning and characterization of the lplA gene and gene product. *J. Biol. Chem*. 269, 16091−16100
28. Mulliez, E., et al., On the role of additional [4Fe–4S] clusters with a free coordination site in radical-SAM enzymes. *Front. Chem*., 2017. **5**: p. 17.
29. Navarro-Sastre, A., Tort, F., Stehling, O., Uzarska, M., Arranz, J., Del Toro, M.,. . Lill, R. (2011). A Fatal Mitochondrial Disease Is Associated with Defective NFU1 Function in the

Maturation of a Subset of Mitochondrial Fe-S Proteins. *The American Journal of Human Genetics*, *89*(5), 656-667. doi:10.1016/j.ajhg.2011.10.005

30. Nesbitt, N. M., Baleanu-Gogonea, C., Cicchillo, R. M., Goodson, K., Iwig, D. F., Broadwater, J. A., Haas, J. A., Fox, B. G., and Booker, S. J. (2005) Expression, purification, and physical characterization of Escherichia coli lipoyl(octanoyl)transferase. *Protein Expression Purif.* 39, 269−282.
31. Packer, L; Witt, EH; Tritschler, HJ (August 1995). "Alpha-lipoic acid as a biological antioxidant". *Free Radical Biology and Medicine*. **19** (2): 227–50.
32. Pandelia, M., Lanz, N. D., Booker, S. J., & Krebs, C. (2014). Mössbauer spectroscopy of Fe/S proteins. *Biochimica Et Biophysica Acta*, 1395-1405. Retrieved January 15, 2021.
33. Py, B., Gerez, C., Angelini, S., Planel, R., Vinella, D., Loiseau, L., Talla, E., Brochier-Armanet, C., Garcia Serres, R., Latour, J. M., Ollagnier-de Choudens, S., Fontecave, M., and Barras, F. (2012) Molecular organization, biochemical function, cellular role and evolution of NfuA, an atypical Fe–S carrier. *Molecular Micribiology*. 86, 155–171
34. Reed, L. J., Koike, M., Levitch, M. E., & Leach, F. R. (1958). Studies On The Nature And Reactions Of Protein-Bound Lipoic Acid. *Journal of Biological Chemistry*, *232*(1), 143-158. doi:10.1016/s0021-9258(18)70382-7
35. Reed, L. J., Leach, F. R., & Koike, M. (1958). Studies On A Lipoic Acid-Activating System. *Journal of Biological Chemistry*, *232*(1), 123-142. doi:10.1016/s0021-9258(18)70381-5
36. Skoog, D. A., Holler, F. J., & Crouch, S. R. (2018). *Principles of instrumental analysis* (6th ed.). Australia: CENGAGE Learning.
37. Zhao, X., Miller, J., Jiang, Y., Marletta, M. A., & Cronan, J. E. (2003). Assembly of the Covalent Linkage between Lipoic Acid and Its Cognate Enzymes. *Chemistry & Biology*, *10*(12), 1293-1302. doi:10.1016/j.chembiol.2003.11.016
38. Lanz, N. D., Grove, T. L., Gogonea, C. B., Lee, K. H., Krebs, C., & Booker, S. J. (2012).RlmN and AtsB as models for the overproduction and characterization of radical SAMproteins.Methods in Enzymology,516, 125–152
39. Zhao, X., Miller, J. R., and Cronan, J. E., Jr. (2005) The reaction of LipB, the octanoyl-[acyl carrier protein]:protein N-octanoyltransferase of lipoic acid synthesis, proceeds through an acyl-enzyme intermediate. Biochemistry 44, 16737−16746.
40. Wachnowsky, C., Wesley, N. A., Fidai, I., & Cowan, J. (2017). Understanding the Molecular Basis of Multiple Mitochondrial Dysfunctions Syndrome 1 (MMDS1)—Impact of a Disease-Causing Gly208Cys Substitution on Structure and Activity of NFU1 in the Fe/S Cluster Biosynthetic Pathway. *Journal of Molecular Biology*, *429*(6), 790–807. https://doi.org/10.1016/j.jmb.2017.01.021

ACADEMIC VITA

Jay Pendyala
jxp5721@psu.edu

EDUCATION

Downingtown STEM Academy ***2013-2017***
International Baccalaureate Recipient
The Pennsylvania State University (*Schreyer Honors College*) ***2017-2021***
Eberly College of Science | Bachelor of Science in Biochemistry and Molecular Biology

MERIT BASED SCHOLARSHIPS & GRANTS

Schreyer Academic Excellence Scholarship	***2017-2021***
David S. Rocchino Family Foundation Scholarship	***2017-2018***
Jack and Frances Tsui Honors Scholarship	***2017-2020***
Undergraduate Research Support	***2018-2019***
Undergraduate Research Support	***2019-2020***
Erickson Discovery Grant	***Summer 2019***
Student Engagement Network Grant	***Spring 2020***
Graham Open Doors Honors Scholarship	***2020-2021***

RESEARCH EXPERIENCE

Boal Laboratory at The Pennsylvania State University ***Aug. 2018- Present***

- Working as an undergraduate researcher with principal investigator Dr. Amie Boal and graduate student Vivian Jeyachandran.
- Performed techniques such as PCR, restriction digestion, bacterial transformation, plasmid purification, bacterial expression, protein purification and crystallographic studies to elucidate the mechanism of Fe-S cluster assembly in the metalloenzyme, LipA, by the Fe-S carrier protein, Nfua.
- Implication of research could contribute to the development of novel therapeutic strategies to overcome disorders such as Friedreich's Ataxia, ISCU myopathy, and sideroblastic anemia.
- Presented posters at the Fall 2019 and Spring 2020 Undergraduate Research Exhibitions
- Recognized as a 2019-2020 Beckman Scholar Finalist

CLINICAL EXPERIENCE

Adult Volunteer at Mount Nittany Medical Center ***Sept. 2019-Mar. 2020 (55.58 hrs)***

- Interact with staff and patients on second, third, and fourth patient floors

- Aid in patient discharge and delivery of mail, flowers, cards, and etc. to patients
- Aid in transport of I.V. pumps and sterile equipment processing
- Aid in transport of placenta to hematopathology lab and blood samples to blood bank

Clinical Observation Student ***Jan.-Mar. 2020 (33.09 hrs)***

- Shadowed Dr. Natalie Tussey, a hospitalist at Mount Nittany Medical Center
- Accompanied and observed Dr. Tussey as she interacts with a spectrum of patients.
- Constantly learning how to handle patient interactions, reason a certain diagnosis, prescribe effective and appropriate treatments, and participate in inter-colleague dialogue to promote quality healthcare

Virtual Pre-Medicine Shadowing ***Jan. 2021-Present (10 hrs)***

- Attend and participate in weekly seminars provided by healthcare professionals on topics such as Anesthesiology, History and Insights to Surgery, Legalities in Medicine, and Forensic Medicine
- Successfully completed post-seminar assessments and certification of completed hours available upon request

Heal Clinical Education Network ***Feb. 2021-Present (5 hrs)***

- Attend clinical education sessions provided by 4th year medical student Mitra Sharifi on topics such as palliative care, pediatric, and surgery.
- Engage in discussion using cases from The ReelDx Library, take SOAP notes and apply critical reasoning towards differential diagnosis.
- Successfully complete homework assignments
- Certification of hours will be acquired after successful completion of the monthly modules and available upon request

EXTRACURRICULAR ACTIVITIES

Schreyer Student Council ***Sept. 2017-May 2018***

- Member of the Merchandise Committee.
- Suggested and helped finalize a variety of apparel to implement into the collection.
- Helped organize Founder's Day Sale, Homecoming Sale, Winter Sale, and Accepted Students Program. Sold over $8000 worth of merchandise

Alpha Epsilon Delta (AED) ***Jan. 2019-Present***

- Member of a nationally recognized pre-professional health club that aids college students aspiring for a career in healthcare
- Participate in THON (a childhood cancer awareness event) fundraising, and various on and off campus service events.
- Mentor underclassmen interested in medical school through the Peer-Mentoring Program
- As Spring 2020 Service Subchair promoted the involvement of members in Centre Volunteers in Medicine, organization that provides primary medical and dental care to underserved patients in Centre County, PA
- Proposed cooperation with Remote Area Medical Club (RAM) to further their pre-existing out-of-state efforts to provide free services to those who are unable to afford medical care themselves and do no have healthcare facilities in their area

Learning Assistant for Math 140B ***Aug.- Dec. 2018***

- Provided instructional assistance for Dr. Andrew Baxter's Math 140B course

- Helped students with Calculus I concepts during class 3 times a week
- Held weekly study sessions outside class to help students in Calculus I with biological applications

Teaching Assistant for Microbiology 201 ***Jan.-Feb. 2019***

- Provided instructional assistance for Dr. Timothy Miyashiro's Microbiology 201 course
- Helped students on concepts such as microscopy, microbial growth, and prokaryotic/eukaryotic cell structure and function

Learning Assistant for Chemistry 212 ***Aug.-Dec. 2019***

- Provide instructional assistance for Dr. Joseph Houck's Chemistry 212 course
- Helped students during class with concepts such as spectroscopy and reaction mechanisms
- Held a weekly 1-hour LA session and an interactive 75 min workshop apart from class

Learning Assistant for Chemistry 210 ***May-July 2020***

- Provide instructional assistance for Dr. Joseph Houck's Chemistry 210 course via Zoom
- Helped students during class with concepts such as identifying electrophilic and nucleophilic sites within compounds and explaining mechanisms of organic reactions for familiar and new addition, substitution, or elimination reactions
- Assisted in an interactive twice weekly 1-hour LA sessions apart from class

Teaching Assistant for Biochemistry and Molecular Biology 460 ***Jan-April 2021***

- Provide instructional advice to Dr. Shawn Xiong's BMB 460 course
- Help students navigate and facilitate discussion of publications on topics such as cell cycle & death, Hippo pathway, TGF-SMAD, Jak-Stat, MAPK, mTORC pathways, stem cells and metabolism.
- Hold a weekly 1-hour office hour in addition to the lectures/journal clubs
- Assisted in creation of problem sets for the Stem Cell portion of course.

WORK/EMPLOYMENT

JustTennis Coach ***Mar. 2017-Aug. 2019***

- Coached 6-14 age kids at various locations throughout the week, helped oversee 8U and 12U tournaments on the weekend for a local tennis company called *JustTennis*.
- Trained 14-17 age students trying out for their respective high school teams

Chemistry Grader ***Jan. 2019-Dec. 2019***

- Spring 2019: Worked as a grader for Dr. Katherine Masters' Chemistry 212 course
- Fall 2019: Worked as a grader for Dr. Joseph Houck's Chemistry 212